Ultrafast meets ultrasmall: controlling nanoantennas and molecules

Lukasz Piatkowski[1]*, Nicolò Accanto[1] , Niek F. van Hulst[1,2]*

[1] ICFO—Institut de Ciencies Fotoniques, The Barcelona Institute of Science and Technology, 08860 Castelldefels (Barcelona), Spain.

[2] ICREA—Institució Catalana de Recerca i Estudis Avançats, 08010 Barcelona, Spain.

Supporting Information Placeholder

ABSTRACT: We present a review on the advances of pulse control and ultrafast coherent excitation of both plasmonic nanoantennas and individual molecular systems, primarily based on the achievements in our group. Essential concepts from coherent control of ultrashort broadband laser pulses are combined with nanoscale diffraction limited detection and imaging of single photon emitters, i.e. the central area of this work is where ultrafast meets ultrasmall. First, the critical role of dedicated pulse shaping and phase control is discussed, which is crucial to realize free of spatio-temporal coupling Fourier limited pulses inside a high numerical aperture microscope at the diffraction limited spot. Next we apply this scheme to plasmonic antennas, exploiting broadband two-photon excitation, to determine amplitude and phase of plasmonic resonances, to achieve ultrafast switching of nanoscale hotspots, and multicolor second harmonic detection for imaging applications. Subsequently we address single molecules with phase-shaped pulses to control the electronic state population and retrieve single molecule vibrational dynamics response. We compare the response of a molecule to phase-locked with free phase multipulse excitation. Furthermore, we discuss phase control of excited state energy transfer in photosynthetic molecular complexes. Finally we combine nanoscale plasmonics with single molecule detection, to attain strong enhancement of both excitation and emission, with fluorescence lifetime shortening to the ps range. In conclusion, we anticipate that this review on ultrafast plasmonics and single emitter control will provide a useful view of the status of ultrafast nanophotonics and its application potential.

KEYWORDS: plasmonic nanoantenna, single molecule, coherent control, pulse-shaping, pump-probe, ultrafast nanoscopy

The experimental study of light-matter interactions at the level of individual nano-objects, to address fundamental spectroscopic properties beyond ensemble average is now routine in many laboratories. Single molecules, semiconductor quantum dots (QDs), metallic nanostructures are readily studied with a wide variety of optical techniques. In parallel, the field of ultrafast lasers has also developed strongly in the past two decades. Today, broadband lasers capable of delivering 15 fs pulses are used by many research groups for the study of the ultrafast processes and coherent dynamics in a large variety of systems. Bridging these two fields, the ultrasmall and ultrafast, is the current challenge in nanophotonics. The capacity to investigate femtosecond dynamics on the single nano-particle level is promising to disentangle dynamical processes such as the intra-particle energy redistribution and inter-particle energy transfer, which govern the ultrafast dynamics immediately after the absorption of a photon; or to examine the electronic dephasing and coherent processes associated with resonances in single molecules, QDs and plasmonic nano-particles.

Even though both single molecule detection[1-5] and femtosecond spectroscopy in the condensed phase[6-10] were thriving already in the '90s, it was not until after the year 2000 that the two fields gradually merged together and the first ultrafast microscopy of individual QDs[11] and molecules[12] was realized. The field of ultrafast nanophotonics is therefore quite recent and many research groups are currently developing new experimental strategies in this direction.[11,13-25]

Our group has been active in the past 10 years on the ultrafast and coherent investigation of single molecules[12,26-32] and nanostructures, with particular focus on plasmonic nanoantennas.[28,33-36] Our objective has not only been to understand, but also to actively control ultrafast dynamics in individual nanoparticles. With the faster-than-ever progress in

nanophotonics and nanotechnology and our growing ability to manipulate nanoscale dynamics, we might one day gain full control of the essential intra- and inter-particle dynamical processes at the single nano-particle level.

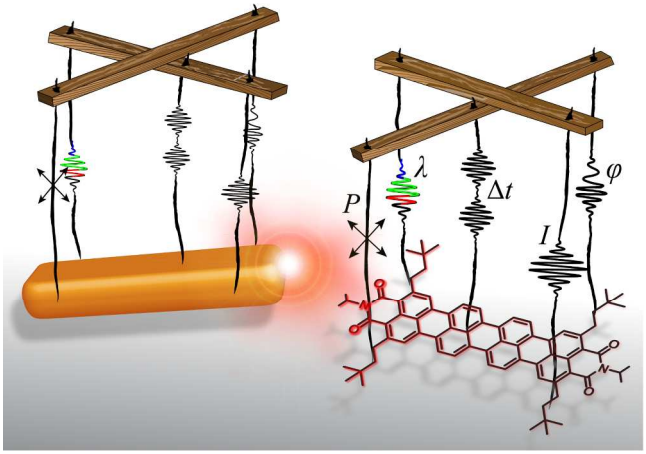

Figure 1. Puppetry vision of the ultrafast coherent nanoscopy. By pulling the coherent control strings, the dynamics of nanoantennas, molecules and their interactions can be orchestered.

In experiments, the study of ultrafast light-matter interactions essentially comes down to delivering a specific series of ultrashort laser pulses with defined properties to the desired sample area and detecting relevant responses (observables) of the sample. One draws conclusions about the sample dynamics by manipulating one (or a few at the same time) of the accessible parameters of the ultrashort pulses: intensity, phase-time relation (chirp, pulse duration), color (and bandwidth), pulse sequence or polarization. Each of the laser pulse handles gives access to particular information: excitation power dependence (I), spectral position of resonances and relative excitation efficiency (λ), dynamics (Δt), anisotropy and mode directionality (polarization, P) and finally temporal resolution/coherent effects (intra-pulse and inter-pulse spectral phase, φ and ϕ). The aim is to eventually be able to actively induce the desired change in the sample in a controlled way. An analogy to puppetry can be drawn here (see Fig. 1). In the learning stages one pulls one string (parameter) at a time and looks at the response of the puppet. Once knowledge of which string leads to what movement is acquired, one knows exactly in what harmony, order, direction and strength to pull the strings to obtain the desired movement, to make the puppet dance for instance.

In a simple picture, the ultrafast response of a molecule or a nano-particle to a photon excitation can be divided into two parts: the coherent and the incoherent regimes, which pertain to different timescales and therefore have different experimental requirements. In the coherent regime the nano-particle is sensitive to the phase properties of the excitation field. A properly designed pulse sequence, with tailored phase relation can therefore be used to control the response of the system, a concept that is usually named *coherent control*.[37-42] In molecules at room temperature however, the coherence is very short lived, typically on the order of few 10s of femtoseconds, due to a large number of (coupled) degrees of freedom and strong coupling to the environment. Hence accessing coherent dynamics requires ultrashort phase-controlled pulses. After the coherent regime, the system relaxes incoherently towards the equilibrium. The initially created population in the electronic excited states relaxes down the vibrational ladder to the lower lying vibrational states, a process termed (in case of molecules) intramolecular vibrational relaxation (IVR).[43] This typically occurs on a picosecond timescale. The particle then returns from the lowest excited state to the ground state through spontaneous emission within nanoseconds (with a probability given by the internal quantum yield).[1,44] In this regime the particle is insensitive to the phase of the laser pulse with which it interacts.

In this review we summarize our efforts in understanding and manipulating these different ultrafast regimes in both single molecules and plasmonic nanoantennas. The practical realization of these experiments is challenging, and the spread of ultrafast and ultrasmall studies throughout various research groups depends on the availability of a well-controlled experimental approach. In this review we therefore give special attention to the realization of a robust and easy to operate experimental platform for the study of ultrafast nanoscale dynamics. The method we chose for looking at single nano-particles is confocal microscopy, which is a widespread and powerful technique.[45,46] All the experiments described in this review were based on the combination between confocal microscopes and ultrashort laser pulses. For all experiments the appropriate laser beam was coupled into an inverted microscope and focused on the sample with an oil-immersion high numerical aperture (NA) microscope objective. The samples were raster-scanned using a piezoelectric scanner. The generated second harmonic, two-photon photoluminescence or fluorescence signals was collected in epi-confocal geometry and detected with a single-photon counting device for intensity imaging or electron multiplying charge coupled device (EM-CCD) camera for spectral detection. For detailed description of the experimental methods we refer to original publications. The experiments involving phases and coherences were performed with the use of pulse shapers as active elements for controlling the phase of the laser fields.

1. Incoherent dynamics in a single molecule

Our endeavors in studying ultrafast dynamics in individual particles began in 2005, when we adapted the ultrafast transient pump-probe technique, commonly used for ensemble measurements, to address for the first time the incoherent dynamics in single molecules at ambient conditions[12,26]. To this end, we used laser pulses with time duration of about 280 fs, derived from a Ti: sapphire oscillator and pulse-picked to a repetition rate of 1 MHz. The laser beam was propagated through a Michelson interferometer (see Fig. 2a) and split into two parts. The outgoing laser pulse-pair with a mutual delay time Δt irradiated perylene- or cyanine-based molecule (PDI and DiD, respectively) in a confocal microscope. The first electronic transition in the molecule was excited to its saturation to gain access to the excited state energy redistribution dynamics. The experiment was only sensitive to incoherent dynamics for two reasons: the pulses were not short enough to access the coherent regime and the lack of phase stabilization in the interferometer prevented the experiment from accessing phase information. The intensity of the laser was set such that a single excitation pulse drove the target transition to saturation, meaning that there was the same 50% probability for the molecule to be promoted to an excited state or to be stimulated back to the ground state by the same pulse. Assuming that the quantum efficiency for the studied molecules is close to unity this implies that the chance of emitting a fluorescent photon was also 50%. The presence of the second, probe pulse at the same time (Δt=0) would not increase the probability for the molecule to end up in the excited state. Also if the molecule would remain in the same excited vibronic state (or superposition of states) for a long time $\tau >> \Delta t$ the interaction with the second pulse would not affect the chance to excite the molecule to the excited state. In this case the fluorescence signal would remain constant as a function of the inter-pulse delay time Δt. This balance however is broken when the lifetime of the excited state is short, that is hundreds of femtoseconds to few picoseconds. If the energy gets redistributed amongst other vibrational states in the excited electronic manifold, the excited state population becomes out of resonance with the second laser pulse. Therefore the probability for the second pulse to stimulate the molecule to the ground state decreases with a timescale of the initially excited state lifetime τ_{ER} and the molecule has a bigger chance to remain in the excited state. Consequently the probability of emitting spontaneous photons increases (up to a maximum of 75%). This is reflected in the modulation of the measured fluorescence signal as a function of Δt: at Δt=0 fluorescence signal is smaller than it is at longer delay times. The onset of the redistribution dynamics of the initially excited vibrational modes to other vibrational modes is directly encoded in the change (around Δt=0) of the inter-pulse delay time-dependent fluorescence traces, examples of which are shown in Fig. 2c. The red line is a result of the convolution of the energy redistribution time τ_{ER} with the auto-correlation of the excitation pulse.

The observed ultrafast energy redistribution may in principle involve two processes: the *intramolecular* vibrational relaxation (IVR)[43] and/or *intermolecular* energy transfer between the fluorophore and the encapsulating polymer molecules.[47] Structural and orientational diffusion are ignored here as they typically occur on a much longer time scale (few ps).[48] The extracted energy redistribution dynamics for the two investigated molecules (PDI and DiD) in the same polymer matrix were different. On the other hand, encapsulating DiD molecule in two different polymer matrices (PMMA or Zeonex) had only a minor effect on the extracted dynamics. Based on these findings we determined that it is the *intramolecular* inter-state relaxation that determines the observed dynamics and that the intermolecular coupling is of less importance here. Interestingly we found that the extracted relaxation times are independent of the exact excitation wavelength for both molecules (DiD and PDI) under study (see Fig. 2d). This implies that on average the same relaxation pathways were probed for individual molecules. The large distribution of the extracted relaxation rates (~20-400 fs) indicates a significant heterogeneity in conformation and local environment and consequently the intramolecular vibrational mode coupling among individual molecules.

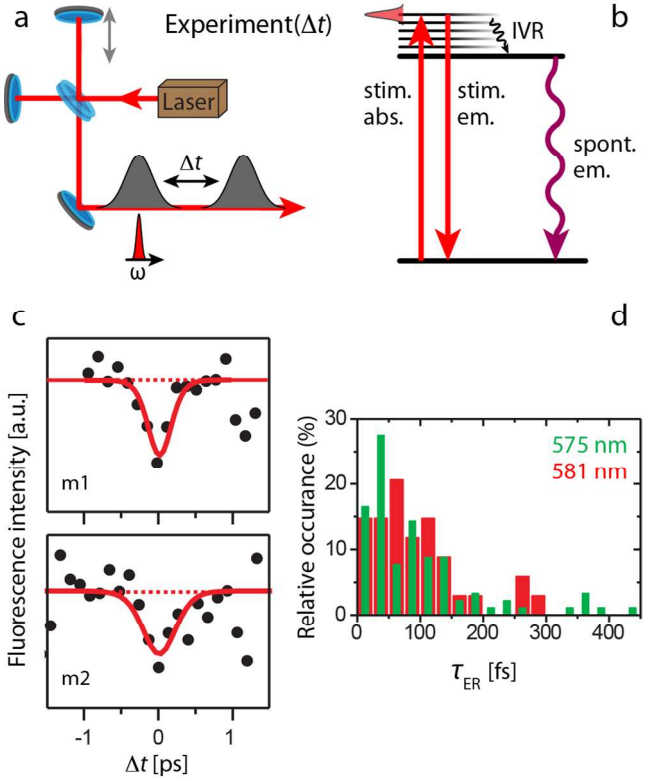

Figure 2. (a) Schematic of the *incoherent single-color* pump-probe experimental setup. (b) Concept of the experiment: inter-pulse delay time-dependent fluorescence signal provides information on the intramolecular vibrational relaxation (IVR) dynamics. (c) Typical fluorescence pump-probe traces for two individual molecules m1 and m2. (d) Histogram of the energy redistribution times τ_{ER} in PDI molecules for two different excitation wavelengths.[12,26]

The discussed pump-probe scheme can be extended from a single color scheme to a two-color scheme where the probe beam is Stokes-shifted and spectrally overlaps with the emission spectrum of the molecule.[27] In this case the probe (or "dump") beam can stimulate the excited molecules down to the ground state leading to a decrease (depletion) in the spontaneous fluorescence signal, a process that underlies STED microscopy.[49,50] Since the dump pulse can stimulate down only when the molecule is in the excited state, the fluorescence depletion dynamics reflects the excited state population lifetime. However, appreciable excited state depletion was only obtained for rather long, stretched dump pulses (~4 ps) and thus the experiment missed out on any dynamics occurring on a faster time-scale.

These experiments demonstrated that it is possible to probe the ultrafast dynamics in individual molecules at ambient conditions using an incoherent pump-probe technique in combination with confocal detection of the fluorescence signal. However, as already noticed, several limitations are inherent to this experimental approach. First, the finite spectral bandwidth of the laser field limits the temporal resolution of the experiment. It should be noted, however, that the use of much shorter pulses implies the loss of specificity as to which vibrational states are excited (because the broader spectral width of the pulse leads to excitation of multiple vibrational levels and averaging of state-specific dynamics). Second, the lack of a fixed phase relation between the pump and probe pulses prevents accessing coherent effects, which for large molecules at ambient conditions occur typically on a few 10s of fs.[51] Finally, exciting the molecule in saturation leads to fast photobleaching, hence limiting the measurement time.

The next logical step is to set up an experiment with the capability of addressing the coherent regime in the study of single molecules and nano-particles. This essentially means that shorter pulses with active phase control need to be used.

2. Phase control of femtosecond pulses

A necessary prerequisite for the study of coherent ultrafast dynamics at the nanoscale is to have precise control of ultrashort pulses with a spatial resolution comparable to the size of the nano-objects under study. Two fundamental problems arise when trying to achieve such a control in the focus of a confocal microscope.

(i) Ultrashort broadband pulses suffer from large phase/time distortions when propagating through optical components, in particular high numerical aperture (NA) microscope objectives[52]. Quantifying and compensating for the phase distortions is paramount.

(ii) The spatial resolution achievable with confocal microscopes is intrinsically limited by diffraction, whereas molecules and single nano-objects are sub-wavelength in size. Beating the diffraction limit is necessary to obtain nanoscale control of ultrashort pulses.

In a recent work we experimentally addressed these difficulties and demonstrated a general method that enables pulse control in a confocal microscope with high spatial and temporal resolution[34]. The main idea of our approach is to use small nano-probes of deep sub-wavelength dimensions to extract information on the laser spectral phase and to overcome in a single experiment all the obstacles inherent to ultrafast (coherent) microscopy.

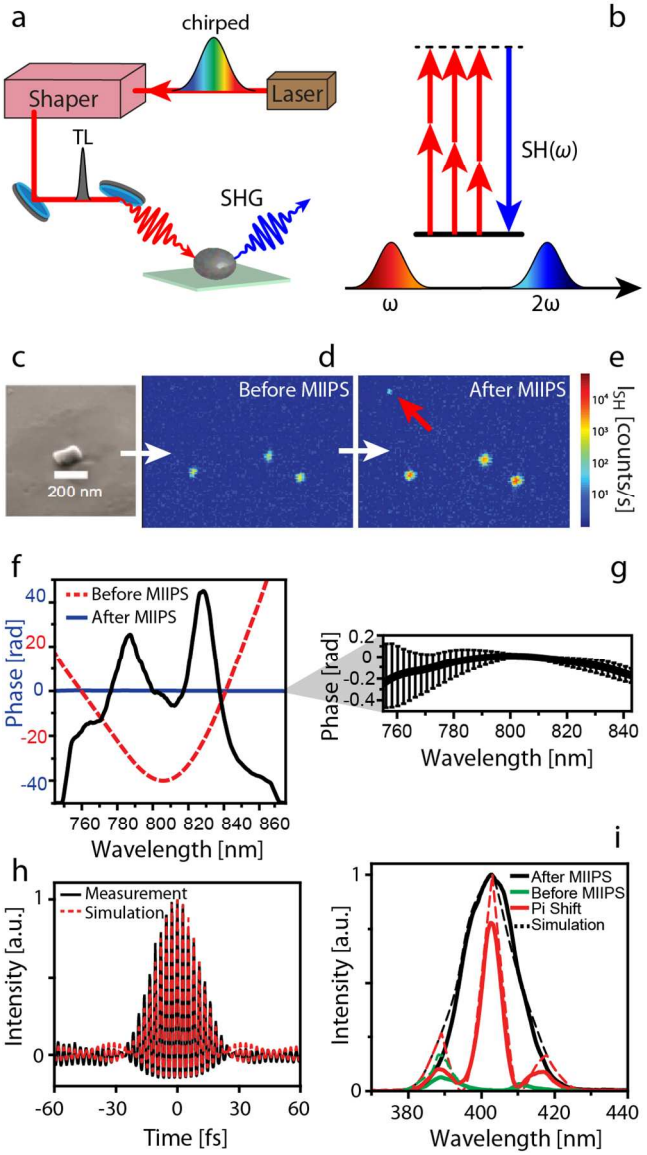

Figure 3. (a) Schematics of the pulse compression experiment on the nanoscale. (b) SHG from a broadband laser involving several different pathways. (c) Scanning electron microscope image of a $BaTiO_3$ NP. Panels d-e show SH images of the same sample area before and after pulse compression, respectively. (f) Laser spectrum (black) and the spectral phase before (red dashed) and after (blue) pulse compression. (g) Mean spectral phase resulting from 15 individual NP measurements. (h) Experimental interferometric autocorrelation of the laser pulses after compression (red dashed) and the simulated one (black). (i) SH spectrum before and after compression and with a pi shift in the spectral phase applied at the center of the laser spectrum (solid lines) and the corresponding simulated spectra (dashed lines).[34]

The nano-probes of the spectral phase were second harmonic (SH) nanoparticles (NPs) of different materials: barium titanate ($BaTiO_3$), iron iodate ($Fe(IO_3)_3$) and gold (Au). When selecting the NPs for this particular application, it is strictly necessary that the particles do not present any resonance at the laser frequency, so they behave as probes, without further affecting the exciting spectral phase. Second harmonic generation (SHG) is widely used for femtosecond pulse characterization in particular with frequency-resolved optical grating (FROG)[53]; spectral phase interferometry for direct electric-field reconstruction of ultrashort optical pulses (SPIDER)[54]; multiphoton intra-pulse interference phase scan (MIIPS)[55]. The main idea of these methods is that SHG, being a nonlinear coherent process, is sensitive to the spectral phase of the excitation electric field. This can be better understood with the aid of the sketch in Fig. 3b. As a 15 fs laser pulse contains a broad range of frequencies, there are several different pathways that can lead to the same final field at the frequency 2ω. The different fields (frequencies) can interfere together to generate more or less amplitude at the frequency 2ω. Most efficient SHG occurs when all these fields are in phase.

In ref[56] a nano-version of FROG was demonstrated, while in our work[34] we used MIIPS on SH NPs to demonstrate full pulse control on the nanoscale. In the experiment (see Fig. 3a) we used a broadband Ti:sapphire oscillator providing pulses centered at 800 nm with a bandwidth of around 100 nm, at a repetition rate of 85 MHz. The laser beam was propagated through a pulse shaper based on a liquid-crystal spatial light modulator (SLM) and organized in a 4f-configuration.[57,58]

We first acquired SH confocal images of a sample containing $BaTiO_3$ NPs (Fig. 3d) from which the position of the NPs could be inferred. Subsequently we focused on a single SH NP of mean size of 180 nm and performed MIIPS on the nanoscale. In a MIIPS experiment[55] a series of known phase functions are imposed on the laser field using the SLM and the corresponding SH spectra are measured.

Because the phase is varied in a systematic way and the full SH spectral information is acquired, a single MIIPS iteration allows one to measure the spectral phase distortions at the sample position. The SLM is then used to compensate for these distortions and compress the pulse in time. In the case of our experiment[34], this resulted in more than one order of magnitude increase in the SH intensity, which allowed imaging even smaller NPs (Fig. 3e, red arrow). In Fig. 3f we report the measured phase before and after MIIPS compression, showing that a flat spectral phase was eventually obtained, even when starting with a highly distorted one. Repeating the measurement on 15 individual NPs yielded the same compression level (reflected in the small standard deviation in Fig. 3g), demonstrating great reproducibility and independence of the specific particle used.

We independently confirmed the accomplishment of pulse compression on the nanoscale by measuring

interferometric autocorrelation traces (Fig. 3h), from which we inferred pulse durations as short as 17 fs. Because in a typical pulse shaping experiment one also desires to control and manipulate at will the spectral phase of the pulse, in the same experimental work we applied a set of spectral phases on the SLM and compared the resulting SH spectra from individual NPs to the simulated ones. In all cases we found good agreement between theory and nanoscale experiment (Fig. 3i).

These results demonstrate our ability to precisely control ultrashort laser pulses, in the phase and time domain, in the focus of a confocal microscope and with high spatial resolution. At the same time they provide an easy to use method for getting started with the investigation of ultrafast dynamics of single nano-objects in the coherent regime.

3. Intermezzo 1 – pulse control hurdles

Let us take a short detour here. As already mentioned, the investigation of ultrafast (coherent) dynamics involves sending a tailored sequence of ultrashort pulses to a certain area of the sample and recording a certain observable while changing the experimental parameters, such as the inter-pulse delay or the laser spectral phase. In the cases described in the rest of this review, these experimental parameters are always controlled through the pulse shaper. It is then crucial that the pulse shaper itself does not introduce any additional experimental side effects when changing the experimental parameters.

In one of our previous works we showed that the degree of control of ultrashort pulses on the nanoscale can be hindered by the presence of spatio-temporal coupling.[28] Shaping of ultrashort laser pulses is typically done by dispersing the beam with a diffraction grating and then acting on each color separately, using for instance the SLM. The inability to precisely recombine all the colors may lead to experimental artifact, which we generally refer to as spatio-temporal coupling[59,60]. The problem with this kind of artifacts is that they heavily depend on the specific configuration of the SLM. A reconfiguration of the SLM, as the one required to change the laser spectral phase or the inter-pulse delay, in general produces different laser beams at the output of the pulse shaper.

In reference[28] we used gold nanoparticles with a diameter of ~100 nm to probe the spatio-temporal coupling in the focus of a confocal microscope. As the size of the NP was smaller than the diffraction limit, scanning the NP across the focal profile and performing simple single color pump-probe experiments allowed us to determine the extent of spatio-temporal coupling. Depending on the position of the NP within the focal spot, the photoluminescence signal from the gold NP showed strong variation as a function of the inter-pulse delay, for the shaper configuration used. This was a consequence of a variation of the focal width and changes in the symmetry of the focal beam profile with the inter-pulse delay Δt.

Fortunately, the observed spatio-temporal distortions can be largely eliminated by adapting the configuration of the shaper.[61] Instead of out-coupling the beam after two passes through the active element the beam is reflected back into the shaper so effectively it passes through an active element four times. We reconfigured our shaper and tested this approach at even higher spatial resolution (few nanometers) by using individual DNQDI molecules. We scanned the molecule across the focal spot and recorded fluorescence intensity traces as a function of inter-pulse time delay. We found that placing the molecule at various positions within the focal spot yields exactly the same modulation in the fluorescence signal, indicative of fully homogeneous focal profile irrespective of the applied inter-pulse delay.

It is evident that, by using molecules, the pulse focus can be investigated with regard to spatio-temporal coupling. However, the use of small nonresonant SH NPs is more efficient as at the same time it enables one to compress femtosecond pulses to their Fourier-transform limit, control the spectral phase of laser pulses with high fidelity and characterize the focal spot of the laser beam - all crucial requirements for the well-controlled ultrafast nanoscopy experiment.

It is worth mentioning here that the use of small NPs is also beneficial for characterization of the aberration of the optical elements, in particular the microscope objective. In ultrafast pump-probe experiments, either single or double color broadband pulses are used with spectral bandwidths of tens to hundreds nm. It is important to ensure that all the wavelengths overlap in the same focal volume to ensure efficient interaction with the system under study. Microscope objectives are known to suffer from chromatic aberration, in particular outside the most commonly used spectral range of approximately 500-650 nm. Detecting scattered laser light or SH from small NPs can be used to characterize the focal volume in terms of chromatic aberration. Filtering spectrally narrow bands out of the broadband pulse and recording the scattered intensity/SH in a confocal manner while scanning the NPs along the propagation axis provides a direct check on whether all the colors overlap in the same focal volume.

4. Plasmonic antennas for ultrafast nanophotonics

In the previous section we showed that the use of non-resonant NPs of dimensions smaller than the diffraction limit gives us full control over the spectral phase, and therefore the time profile of a broadband laser pulse with an unprecedented spatial resolution. The logical successive step is then to apply our nanoscale pulse-shaping scheme to resonant NPs, which do have a coherent response.

Plasmonic nanoantennas are particularly promising in this sense as their localized surface plasmon resonances (LSPRs) can be engineered to overlap with laser fields in the visible and near infrared region of the spectrum[62,63], as shown in the sketches in Fig. 4b-d. An important characteristic of nanoantennas is their capability to confine a resonant propagating electromagnetic field in a small volume (hotspot) in the near field of the antenna. Combining this property of nanoantennas, with ultrashort phase controlled laser pulses, the possibility of achieving coherent control of nanoscale plasmonic field was first theoretically predicted.[64] Experimental demonstrations of similar concepts, although neglecting the coherent response of the nanostructures, were also realized.[13,14] Many studies determined the coherence time of surface plasmons in resonant nanoantennas to be in the 15 fs range and therefore at the limit of the time resolution achievable by broadband laser systems.[20,65-68]

In our group we recently carried out a series of experiments aimed at detecting, understanding and making use of the ultrafast resonant response of plasmonic nanoantennas.[33,35,36] These experiments rely on the detection of nonlinear optical signals from the nanoantennas, such as SHG and two-photon induced photoluminescence (TPPL). When a broadband laser field impinges on a resonant nanoantenna, the interaction is most efficient for the laser frequencies that overlap with the LSPR and which are efficiently localized in the hotspot of the nanoantenna. The localized field is therefore a function of both the incoming field and the LSPR. As a consequence, SHG and TPPL, generated in the proximity of the nanoantenna, are both affected by the resonance response (Fig. 4c-d).

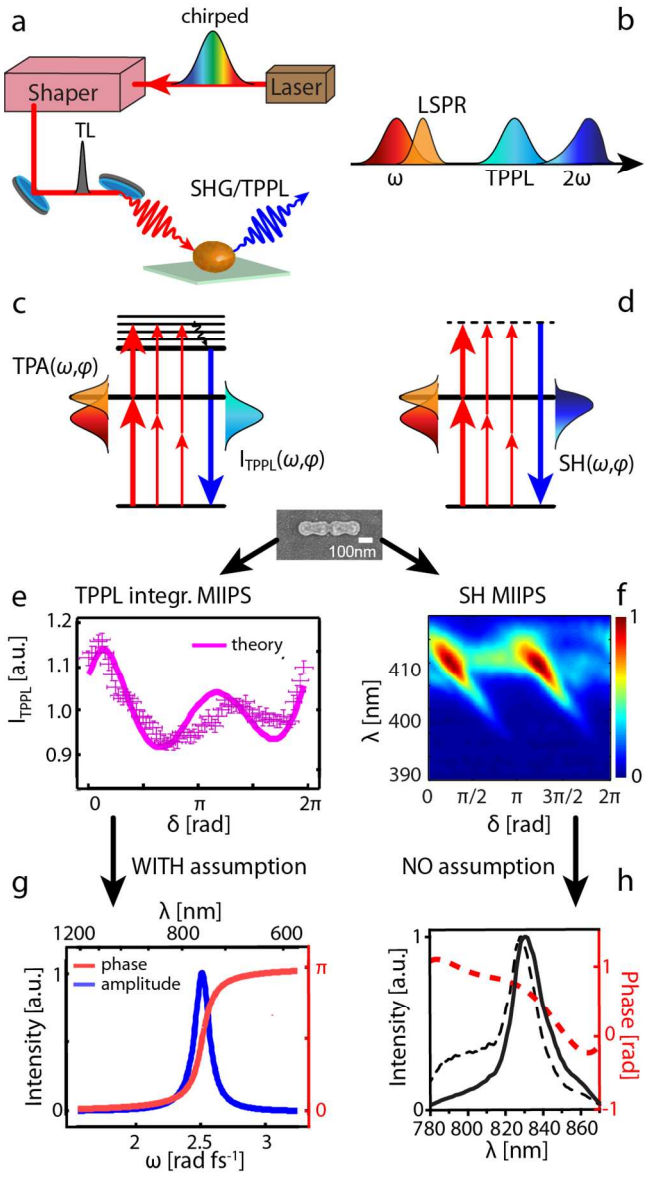

Figure 4. (a) Schematics of the ultrafast nonlinear experiments on plasmonic nanoantennas. (b) Frequency domain representation of a LSPR at the fundamental laser frequency and the TPPL and SHG from a nanoantenna. (c) TPA and TPPL processes in a resonant nanoantenna involving several pathways, with relative importance weighted by the LSPR (thick red arrows). (d) SH processes in a resonant nanoantenna. (e) TPPL intensity MIIPS trace measured on a single nanoantenna and fit to the data based on a Lorentzian response. (f) Spectrally resolved SH MIIPS trace measured on a single nanoantenna (g) Lorentzian phase and amplitude response retrieved from the fit of the TPPL MIIPS trace. (h) Phase and amplitude response and comparison to the laser spectrum, as obtained from the SH MIIPS trace, free of additional assumptions.[33,36]

By observing such nonlinear signals, we first demonstrated that the resonant response of nanoantennas could be measured in its phase and amplitude components[33,35,36]. This is important as the possibility of correctly exploiting LSPRs is subject to the precise

understanding of the effect of the resonances on the incoming laser field. In the experiments we used the nanoscale MIIPS method described above and applied it to individual nanoantennas, detecting either the TPPL intensity[33,35] or the SH spectrum[35,36] (Fig. 4e-f). A fit of the MIIPS traces allows the complete (amplitude and phase) resonant response to be retrieved (Fig. 4g-h). Both experimental approaches present advantages and limitations and the choice of using one or the other should depend on the specific experimental requirement. The main advantage of using the TPPL signal is that it is generally larger and thus more easily detectable than the SH from individual nanoantennas, especially considering that for spectral measurements the SH is divided between several pixels of the EM-CCD camera. However, the TPPL spectrum, unlike the SH, is independent of the laser spectral phase and only its intensity varies as a function of the applied phase. A considerable amount of information contained in a spectrally resolved SH MIIPS trace is therefore lost when detecting the TPPL. As a consequence, an assumption about the shape of the LSPR is necessary to extract information from a TPPL MIIPS trace. In the case of [33] we made the assumption that the nanoantenna response could be well approximated by a Lorentzian function (Fig. 4g), for which both the phase and the amplitude components are different functions of the same two parameters: the central frequency and width of the Lorentzian. In contrast, in the case of SH MIIPS, the full information is contained in the spectrally resolved traces and no additional assumption is needed. In[36] we showed that, in the case of simple nano-rod antennas, the results obtained were compatible with a Lorentzian model, confirming the agreement between the two methods for this simple case. Nevertheless, for an arbitrary and more complex plasmonic structure, for which an accurate prediction on the shape of the resonance is not straightforward, the SH MIIPS approach is a more powerful method to extract information about the LSPR.

These results demonstrate that, by using ultrashort phase-controlled pulses, together with a reliable characterization method, the effect of LSPRs in nanoantennas can be measured. In order to actively exploit these LSPRs, in[33,35,36] we compared the responses of different nanoantennas resonant with opposite sides of the laser spectrum, subject to precise phase shaping of the laser pulse. We demonstrated two different applications: an ultrafast plasmonic switch[33] (Fig. 5a-b), and a multicolor SH imaging technique[35] (Fig. 5c-d).

In the first experiment, based on the theoretical proposal by Stockman and collaborators[64], we used a pair of coupled nano-rods of different lengths (respectively resonant on the blue and red side of the laser spectrum) to move the localized energy from one side to the other of the plasmonic nanostructure on an ultrafast timescale. By exciting the system with a chirped pulse, in which the blue colors arrive at the sample before the red ones, the two different nanorods were separately addressed, with a switching time of ~100 fs. As shown in Fig. 5a-b, the light localization was probed with a second Fourier limited pulse and the TPPL was used as the experimental observable. Correctly designed plasmonic structures combined with the ultrashort laser pulses used to excite them have the potential to generate switchable hotspots with high temporal resolution and highly confined energy. This idea can be exploited to selectively excite single molecules at fs time scale within a close packed ensemble using the nanoantennas.

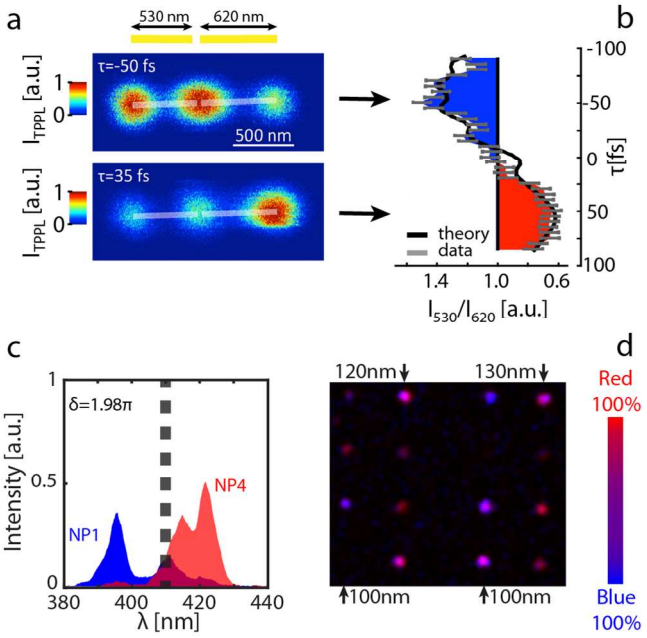

Figure 5. Hotspot switching and multicolor imaging. (a) TPPL image of two coupled nanoantennas excited by a chirped pulse and probed by a transform-limited pulse at two inter-pulse time delays. (b) The luminescent hotspot switches on fs timescale as the chirp runs over the coupled antenna. (c) SH spectral response of two distinct nanoantennas excited by a broadband laser pulse with the spectral phase that maximizes the spectral contrast. (d) Two-color SH image of an array of nanorods: change in the coloring of different nanorods allows us to readily distinguish the rods of different lengths.[33,35]

The second application, illustrated in Fig. 5c-d is a multicolor SH imaging technique.[35] Because the SH spectra from nanoantennas depend on the LSPRs, different nanoantennas in general emit different SH spectra. In a sample that contains two different species of nanoantennas this gives the opportunity to distinguish them based on their SH spectra. This has important implications in biological imaging as it allows one to label different components of a tissue us-

ing different nanoantennas; excite them all at the same time with the same ultrafast laser and then use spectrally selective detection at the SH wavelength to discriminate between the different nanoantennas. A similar experimental technique, often named multicolor imaging, is used regularly to image different fluorescent markers, such as semiconductor QDs, but prior to our work [35] had never been extended to the SH range. In recent works, the possibility of using non resonant SH NPs, such as BaTiO3 NPs, as markers for SH imaging of tissues was considered.[69,70] Benefits of SH imaging include: high stability and absence of photo blinking and bleaching; relatively narrowband emission, allowing for easy spectral separation from the sample auto-fluorescence; use of near infrared excitation, which limits photo-damage of the sample and increases the penetration depth for deep tissue imaging. In our work[35] we showed that, by using resonant nanoantennas together with broadband phase controlled laser pulses, multicolor imaging in the SH range can be achieved. Fig. 5c shows SH spectra from two different nanoantennas, acquired with a specifically tailored spectral phase that maximizes their relative spectral difference. Sending the blue and the red part of the SH (splitting at 415 nm) to different APDs allowed us to discriminate between the two nanoantenna species, as shown in Fig. 5d, which demonstrates the achievement of multicolor SH imaging.

So far we have presented and discussed a toolbox for performing phase-controlled ultrafast experiments on the nanoscale. Plasmonic nanoantennas have provided a good platform to test not only our highly sensitive phase measurement scheme, but also our ability to actively control nanoscale responses. Clearly, these concepts are equally suitable to address single molecule dynamics in the coherent regime. Single molecules under ultrafast phase-controlled excitation are the focus of the second part of this review. The final objective would be to combine molecular and plasmonic systems together and still be able to perform ultrafast coherent control. We will briefly touch on one experiment on single molecules and nanoantennas in the last section of this review.

In the following we demonstrate that having a precise control over the time delay Δt and relative phase $\Delta\phi$ between the pulses allows the study coherent properties of individual molecules and molecular complexes.

In the incoherent pump-probe experiments discussed in the first section, we operated in the excitation saturation regime. Hence in these experiments the interaction of a molecule with the laser light produced an excited state population and excited state population dynamics was reported. Now, in all of the following, rather than limit ourselves to population, we switch to quantum mechanical syntax and address transition probabilities. In these experiments we operate in a weak excitation regime and we exploit quantum coherence, i.e. a state where a single pulse creates a coherent superposition of two or more states in a molecule. Interaction with the second, delayed pulse probes the phase memory of that coherent superposition in time. After the interaction of the molecule with the pulse-pair the probability for the molecule to be in the excited state, becomes a function of both the inter-pulse delay time and phase difference. This leads to a modulation of the excitation probability, which is reflected in a modulation of the fluorescence signal.

One of the holy grails in physical chemistry is the ability to control the behavior of a molecular system. In spectroscopy this implies that the interaction of a molecule with light leads to a localization of the energy in a specific predetermined mode or/and specific energy redistribution pathway or/and specific reactivity pathway. In the experiments presented below the detection and control aspects of the coherence are interrelated and indistinguishable. In fact the detection of the coherence is realized based on the fact that the population probability depends on the inter-pulse phase relation.

5. Detection and control of femtosecond coherence in single molecule

In a simple two-level system, the interaction with a coherent laser field creates quantum coherence between the electronic ground and excited states. This coherence leads to Rabi oscillations, which in simple terms is a periodic change (with the so-called Rabi frequency) of the probability for the molecule to be in the ground or excited state. Rabi oscillations in individual molecules and quantum dots have been detected recently at cryogenic conditions.[71,72]

In our experiment we explored and controlled the coherence in individual terrylenediimide (TDI) molecules at ambient conditions.[32] TDI molecules were resonantly excited at 630 nm with a phase-locked pulse-pair derived from an optical parametric oscillator and the resulting fluorescence was detected in a confocal manner. A pulse picker was used to reduce the repetition rate from 76 MHz to 500 kHz, allowing higher peak power while still providing long observation time of a single molecule before bleaching. The pulses were compressed to their Fourier limit (pulse width of ~75 fs) and, which is crucial for the success of the experiment, the inter-pulse phase relation was precisely controlled using an acousto-optic pro-

grammable dispersive filter (AOPDF) based pulse shaper.

Typical inter-pulse delay dependent fluorescence traces from three individual molecules with Δϕ fixed at 0 rad are shown in figure 6c. The three traces exhibit variation in the fluorescence. The fluorescence counts decrease or increase as a function of the inter-pulse delay time Δ*t* within several tens of femtoseconds, after which they remain constant. The observed dynamics reflects the decay of the coherence between the ground and excited electronic states with a time constant of about 50 fs. The effects of the incoherent excited state relaxation processes are excluded here as they typically occur on much longer time scales (hundreds of fs to ps).[73] The observed turnover from decaying to flat and growing character of the fluorescence trace (top to bottom in Fig. 6c) is attributed to an increased strength of interaction between the transition dipole moment of the molecule and the laser pulse. In other words the laser field drives the transition more effectively and the Rabi frequency increases. The red lines in Fig. 6c represent numerical simulations based on the optical Bloch equations.

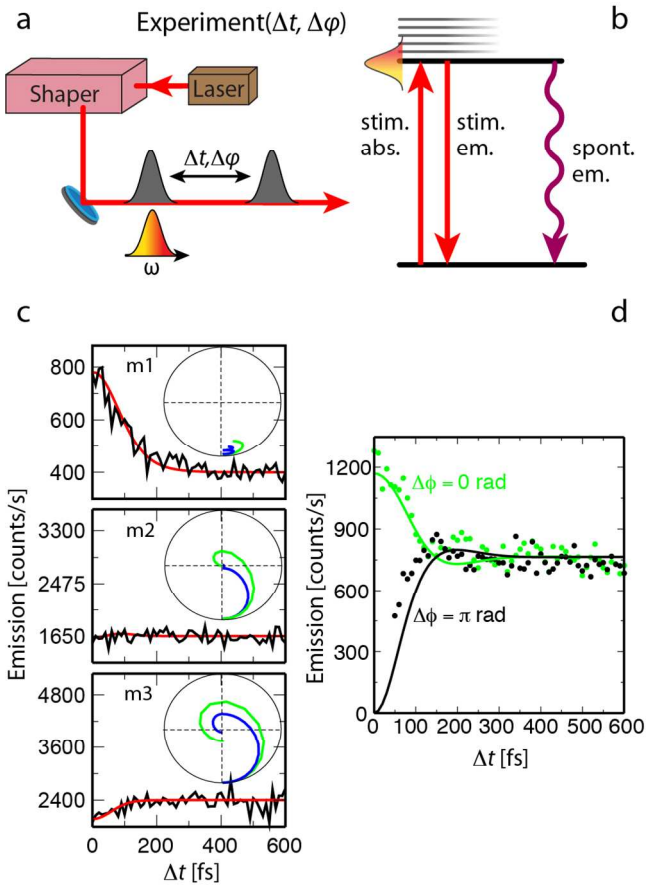

Figure 6. (a) Schematic of the *coherent quasi-broadband* pump-probe experimental setup. (b) Concept of the experiment: an excitation pulse creates a coherent superposition of the electronic ground and excited states, which is subsequently probed with a second pulse. (c) The coherent properties of the molecule are reflected in the inter-pulse delay time-dependent fluorescence traces, providing information on the trajectory of the Bloch vector; green 0 fs time delay, blue 600 fs delay. (d) A π-flip between the two pulses does invert the inter-pulse delay time-dependent fluorescence traces.[32]

The state of a two level system is often represented in the form of a Bloch vector and its evolution is given by the time-dependent trajectories of the vector tip on the Bloch sphere, as shown in the insets in Fig. 6c. In the case of molecule m1 (Fig. 6c, top) the Rabi frequency is small and mainly absorption takes place, while very little stimulated emission. Due to the rapid dephasing, the Bloch vector becomes shorter and the probability for excited state population as a function of Δ*t* decreases. As the interaction between the molecule and the laser field increases (higher Rabi frequency) the trajectories become longer and flip around the Bloch sphere. As a result, the dephasing at larger Δ*t* can leave a higher excited state probability, as in the case of molecules m2 and m3 in Fig 6c. Due to the finite pulse duration (approximately 75 fs) and short dephasing time (~50 fs), complete Rabi oscillation could not be resolved in our data. However, from the calculations (red lines in Fig. 6c) we determined the periods of Rabi oscillations ranging from 20 to 100 fs.

Precise control over inter-pulse phase relation allowed us to manipulate the coherent state of the molecule. The largest contrast was obtained for Δϕ=π, as π phase difference reverses the rotation direction of the Bloch vector hence increases the probability for the molecule to end up in the opposite state, i.e. the ground state. In figure 6d we show two fluorescence traces as a function of the inter-pulse delay time Δ*t* recorded on the same molecule for the inter-pulse phase Δϕ=0 and Δϕ=π rad. Within the coherence time (<100 fs) the in-phase pulse-pair interferes constructively and enhances the excited state population probability (higher fluorescence counts; black data points), whereas the out-of-phase pulse-pair interferes destructively leading to a decrease of the excited state population probability (lower fluorescence counts; green data points).

These experiments clearly demonstrate the ability to prepare a molecule in a specific state. The dephasing time at ambient conditions is very short (<100 fs) and imposes the necessity to use ultrashort pulses. The precision with which we can control the state of a molecule, or in other words the achievable contrast (the molecule resides in the excited or ground state) depends mainly on temporal fluctuations of the interaction strength between the molecule and laser field and the precision with which one controls the

inter-pulse phase. The success of these experiments evidently lies in our ability to control intra- and inter-pulse phase with high finesse.

6. Vibrational wave-packet dynamics in single molecules

In the previous section we discussed the simplest manifestation of quantum coherence between the two electronic levels of a molecule. Other than preparing the molecule in an arbitrary superposition of the two states we demonstrated the ability to enhance or decrease the probability for the molecule to be promoted to the excited state. Exploiting this coherence however does not provide any handles to deterministically steer a molecule to a specific final state out of a multitude of accessible states. It only allows tipping the scale of probability for the molecule to end up in one of the two states (ground or excited).

The next experiment addressed in this review focuses on visualizing and controlling coherence within a single electronic excited state but involving multiple vibrational states.[30] Analogously to previous experiments, also in this work we used a pair of femtosecond pulses with well-controlled inter-pulse delay time Δt and phase shift $\Delta\phi$. The laser pulses were derived from an ultrabroadband Ti: sapphire oscillator, operating at 85 MHz and delivering pulses with a bandwidth of 120 nm, centered at 680 nm. Pulse compression, generation of pulse-pair and control of the inter-pulse phase was performed with a 4f-shaper based on a SLM.

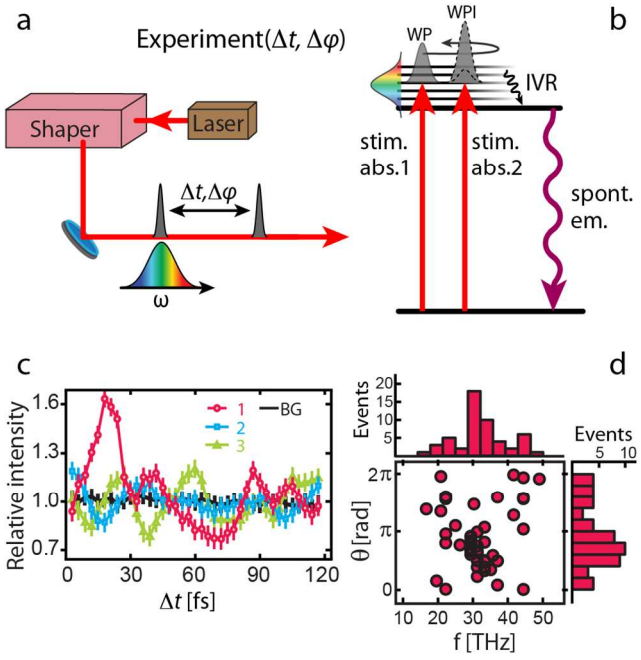

Figure 7. (a) Schematic of the *coherent broadband* pump-probe experimental setup. (b) Concept of the experiment: an excitation pulse creates a coherent superposition of a set of the vibrational states (vibrational wave-packet, WP), which is subsequently probed through an interference with a wave-packet created by the second pulse. The coherent properties of the vibrational wave-packet interference are reflected in the inter-pulse delay time-dependent fluorescence traces.[30]

As a molecule of study we used a rylene homologue called DNQDI[74]. Single molecules were illuminated with a pulse of sufficient bandwidth to excite several vibrational levels in the electronic excited state and thus generate a quantum wave-packet.[75] The excited wave-packet travels in time within the excited state potential back and forth until the phase relation between individual vibrational states (coherence) is lost. The second, delayed, pulse leads to generation of a second wave-packet. If the two wave-packets are generated within the coherence time, quantum interference between them leads to an enhancement or suppression of the excited state population probability and therefore to modulation of the fluorescence intensity. The fluorescence traces as a function of the inter-pulse delay time Δt and fixed inter-pulse phase difference, for three exemplary molecules are shown in figure 7c. The traces are normalized to the fluorescence intensity at long delay times. All traces exhibit oscillatory character with a typical modulation in the order of ±10% of the average fluorescence level. As explained earlier, these oscillations reflect the quantum wave-packet interference. The oscillations with a period of 30-40 fs typically vanish on a timescale of 100 fs, indicative of the wave-packet phase memory loss, i.e. dephasing. Fourier analysis of the fluorescence traces revealed a single, dominant component with a frequency of around 33 THz (see Fig. 7d). The extracted frequency of 33 THz (or 1000 cm^{-1}) reflects the travel time of the wave-packet within the excited state potential and is therefore directly linked to the energy separation of the vibrational states comprising that wave-packet. The variation in the starting phase of the oscillations among individual molecules is attributed to the large heterogeneity of their characteristic vibrational progression, that is spectral positions, widths and strengths.

The generation and in particular control of a vibrational wave-packet gives much more control over the molecule than the inter-electronic state coherence discussed in previous section. We can shape the pulse in frequency domain to form a wave-packet of arbitrary states. Coupling of these states within the vibrational manifold and with extramolecular modes gives plenty of possible energy relaxation and energy transfer pathways. Hence, optimization of the time-phase structure of the exciting pulse-pair can be used to excite individual molecules at ambient conditions to a desired, specific target state.

7. Intermezzo 2 – Inter-pulse phase relation and single molecule excitation spectroscopy

We have just learned that it is possible to launch and probe the evolution of a vibrational wave-packet in a single molecule at ambient conditions provided that the laser pulses have sufficient bandwidth and that we can precisely control the inter-pulse phase relation. The use of the shaper allowed us to keep the relative phase between the pulses fixed at $\Delta\phi$ and scan only the inter-pulse time delay. By changing the phase relation from in-phase ($\Delta\phi=0$) to out-of-phase ($\Delta\phi=\pi$) the phase of the fluorescence trace recorded from the same molecule changes by π as well, as shown in figure 8a. This is a clear demonstration that by tuning the inter-pulse phase we can arbitrarily control the excited state population probability.

An alternative approach is to let the inter-pulse phase $\Delta\phi$ change together with the inter-pulse delay time Δt. Recently we performed such an experiment on individual QDI molecules, where instead of phase-locked pulses, the pulse-pair was generated in a Michelson interferometer using a motorized delay line.[76] The outgoing pulses continuously interfere with each other as a function of the inter-pulse delay time Δt. The interfering pulse-pair excites the molecules and the resulting fluorescence is detected as a function of the inter-pulse delay time Δt. Effectively, different excitation wavelengths are sampled when scanning a time delay between two interfering broadband (over 100 nm) laser pulses. The fluorescence traces exhibit clear modulation on at least two timescales (see Fig. 8b). The fast oscillations with a period of ~2.3 fs (corresponding to the central wavelength of the broadband pulse of 700 nm) result from the interference of the carrier frequency of the two pulses, and superimposed, slower beating signal with a period of about 50 fs. Analogously to Fourier transform spectroscopy, in order to extract the effect of the molecule on the measured fluorescence traces (interferograms) we first recorded an interferogram of the laser itself, Fourier transformed both signals and divided them in the frequency domain. This way we obtained the excitation spectrum of a single QDI molecule. The observed beating frequency in the time-dependent fluorescence traces comes from the beating of the two vibronic bands in the excitation spectrum of the molecule.

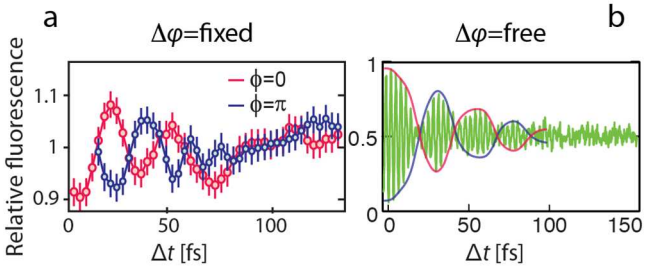

Figure 8. (a) Delay time-dependent fluorescence traces recorded from a single DNQDI molecule for a set inter-pulse phase difference of 0 (red) and π (blue). The observed oscillatory traces reflect the beating due to the vibrational side band.[30] (b) Interferometric fluorescence trace as a function of the inter-pulse delay recorded from an individual QDI molecule.[76]

It should be realized here that even though the two experiments are performed in a different manner: the phase-locked experiment requires a spectral shaper in order to lock the pulses at the central laser frequency; while the interferometric experiment is performed with arbitrary pulses (or CW excitation) and exactly the phase is scanned; the obtained information on the vibrational states is equivalent.[77] Oscillations in the fluorescence signal in the phase-locked experiment reflect the frequency difference of the two beating vibrational bands. In the interferometric experiment we get the full excitation spectrum of the molecule, hence implicitly the frequency difference between the vibrational states that were excited. The interferometric experiment probes the excitation probability of the molecule over the sampled excitation wavelength range, while it does not allow for control over the excited state population.

8. Two-color phase-controlled detection of energy transfer in light harvesting complexes

In the previous sections we discussed experiments that uncover coherent properties in individual molecules: Rabi oscillations and vibrational wave-packet interference. In nature however, complex (molecular) architectures most of the time not only involve modes that are intricately coupled to each other but also involve energy transfer between molecular units. An example of such system is the light harvesting complex 2 (LH2), a biologically relevant macromolecule that is found in purple bacteria. LH2s are the main antenna complexes in the light harvesting process and as such they play a crucial role in photosynthesis. Coherent effects have been observed in LH2 complexes in bulk experiments.[78-80] Consequently it has been speculated that coherent delocalization of the excitation energy may be responsible for the observed high efficiency of the energy conversion in such photosynthetic organisms.

LH2 are complex architectures that, in simple terms, are built of two pigment-protein rings, which give rise to distinct electronic transitions called B800 and B850, according to the wavelengths at which they absorb light (see Fig. 9).[81,82] The energy absorbed by the B800 band is transferred to the B850 band and funneled towards the reaction center. In our experiment we addressed the coherent character of the B800-B850 energy transfer step in individual LH2 complexes.[31] To this end we designed a two-color experiment in which the two transform-limited pulses (pulse duration of ~15 fs) are resonant with the B800 and B850 band, respectively. We detected the fluorescence signal as a function of the time delay Δt between the two pulses, keeping the relative phase between the pulses constant. The pulse-pair used was generated through phase-shaping in the pulse shaper. Evidently, the experiments discussed in earlier sections are of extreme importance here, as the success of this experiment is highly dependent on the control over spectral phase of the ultrashort pulses. Moreover the experiment has to be free of spatio-temporal coupling in order to probe solely excitation-pulse induced effects.

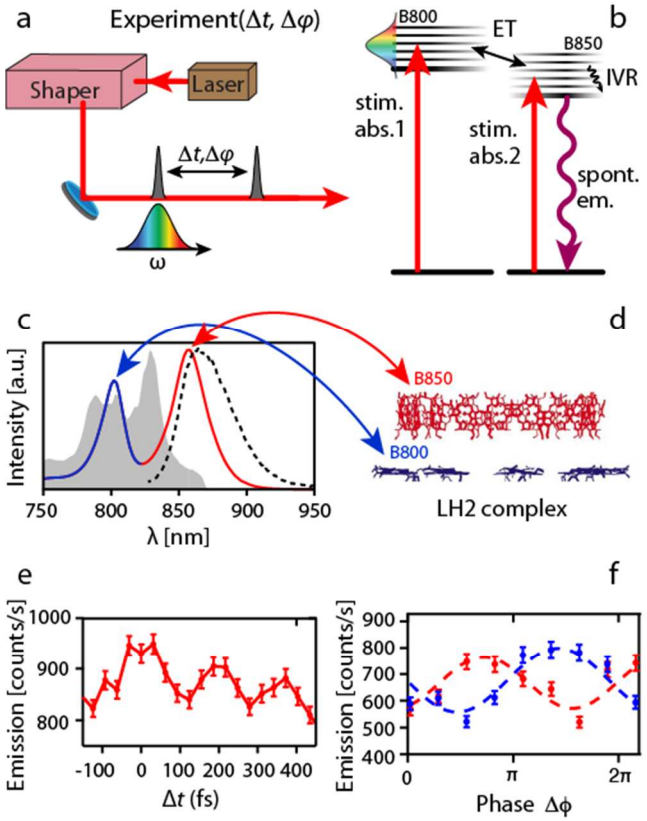

Figure 9. (a) Schematic of the *coherent broadband* pump-probe experimental setup. (b) Concept of the experiment: an excitation pulse creates an excited state population in the B800 band of the LH2 complex. The energy transfer to the B850 band is subsequently probed with a second pulse, resonant with the B850 band. The coherent properties of the intermolecular energy transfer are reflected in the inter-pulse delay time-dependent fluorescence traces. (c) Blue/red line represents the absorption spectrum of the LH2 ensemble solution. Grey, shaded area reflects the laser spectrum. Dashed, black line indicates emission spectrum of the LH2 ensemble solution. Green, solid line is the phase profile applied to the laser spectrum in order to generate a pulse-pair. (d) Simplified representation of the LH2 complex structure. Chromophores are organized in two rings giving rise to the distinct absorption bands, called B800 (blue) and B850 (red). (e) An exemplary inter-pulse delay time-dependent fluorescence trace recorded with a fixed phase difference between the pulses from a single LH2 complex. (f) Phase-sweep traces recorded on the same molecule for a fixed inter-pulse time delay. The red and blue trace result from averaging the first three and subsequent seven consecutive phase-sweep traces.[31]

The measured time-dependent fluorescence traces recorded from individual molecules exhibit oscillations with a period of about 200 fs and lasting over 400 fs (exemplary trace is shown in Fig. 9e). The observed oscillations are ascribed to quantum interference between two excitation paths that populate the same target state, that is the emitting lowest-energy B850 state. The blue-shifted pulse induces excitation in the B800 band, which in time repeatedly acquires character of the B850 band. In other words, the inter-band B800-B850 electronic coupling, possibly assisted by resonant low-energy vibrational modes, make the excited electrons travel back and forth within the coupled B800-B850 potential energy surface. The second, redshifted pulse can then either enhance or reduce the population of the emitting B850 state through quantum interference, thus giving the fluorescence trace its oscillatory character.

Probing the coherence in many individual LH2s we found a rather large spread of the oscillation periods, ranging from 100 to 400 fs. Given the complexity of LH2, the involvement of many modes and contribution from thermal fluctuations, it is understandable that slightly different energy transfer pathways will be optimal for individual complexes.

It is important to note here that the coherence in this particular energy transfer process on average persists much longer (>200 fs) than a typical coherence in isolated fluorophore in polymer matrix (~50 fs).[32,44] Even though the intrinsic strength and typical timescale of the coherence differs among complexes, the robustness of the inter-mode coupling in combination with the extensive protective protein scaffold appears to effectively screen the two modes from coupling to other energy dissipation channels.

Finally we attempted to influence the final fluorescence probability of a single LH2. Sweeping the inter-pulse phase relation between 0 and 2π at constant time delay between the two excitation pulses Δt=100 fs lead to oscillatory traces indicating that we can externally influence the efficiency of populating

the emitting B850 state (see Fig. 9f). So here once again it is important to have full time and phase control over the laser pulses – otherwise it is impossible to carry out such an experiment.

By repeating the phase sweep (0-2π) scan multiple times on the same complex we found that the phase of the measured oscillatory fluorescence signal changes occasionally on a timescale of some 10s of seconds (red and blue trace in Fig. 9f). Apparently, even within the same complex different energy transfer pathways can dominate at different times.

In the experiments highlighted in the two previous sections we probed and controlled the final excited state population in individual molecules. The experiment described here forms yet another step towards the ability of steering the chemical reactions at a single molecule level, as we are effectively able to control the energy transfer efficiency between spatially distinct multi-molecular rings within one LH2 complex. These pioneering experiments pave the road for investigation of other ultrafast energy transfer and delocalization processes on the nanoscale.

9. Intermezzo 3 - molecules meet plasmonics

The detection of single molecules and the investigation of molecular dynamics through fluorescence is still the most common choice in laboratories around the world as it typically delivers a superb signal-to-background ratio. However, in many cases, such as for the LH2 complexes, fast photobleaching, low fluorescence quantum efficiency and ultimately the limited fluorescence photon budget hinder progress in the investigation of ultrafast dynamics at a single molecule level at ambient conditions.

It has been demonstrated that plasmonic nanoantennas can boost the brightness of fluorophores by concentrating the electromagnetic fields into sub-diffraction limited volumes.[83,84] Coupling of the emitter (a molecule or a quantum dot) to a plasmonic nanoantenna leads to an increase of the excitation efficiency of the emitter and the modification of its radiative and non-radiative rates, which can increase the overall quantum yield of the emitters.[85]

Recently we investigated the properties of LH2 complexes coupled to plasmonic antennas.[86] Even though the experiments are not time-resolved, in the light of this review it seems appropriate to discuss them since with these experiments we took the first steps towards studying ultrafast processes in coupled plasmonic-molecular systems[86]. Briefly, LH2 complexes were spin-coated on a microscope slide with gold nanorod antenna arrays, with a concentration that yielded only a few LH2 complexes per antenna. For optimal fluorescence enhancement both excitation enhancement and quantum efficiency (QE) enhancement are important. Therefore the antenna length of 160 nm was chosen because its gold plasmon resonance overlaps well with both the absorption (800 nm) and emission band (900 nm) of the LH2. The molecules were excited at 800 nm with ~100 fs pulses in a confocal microscope and the resulting fluorescence detected with a single-photon counting device.

Confocal images of the LH2 complexes were recorded with and without the presence of the antenna array. Images were then normalized to the excitation power and the fluorescence counts were directly compared. We found an over 500-fold fluorescence enhancement for LH2 complexes coupled to a gold nanoantennas. Further analysis revealed that the resonant antenna produces an excitation enhancement of roughly 90 times and a fluorescence lifetime shortening to about 20 ps (from the initial ~1 ns). At the same time, the radiative rate enhancement results in a 5.5-fold-improved fluorescence QE. The correlation between the fluorescence enhancement factor and the fluorescence lifetime for a number of investigated molecules is shown in figure 10b. For the >500 times enhanced LH2 complex, the total count rate per molecule was 15 times increased compared to the unenhanced case. This significant increase in the total fluorescence photon budget allowed us to record photon antibunching of a single light-harvesting complex under ambient conditions, revealing that this multi-chromophoric complex behaves as a non-classical single-photon emitter.

Evidently the presented approach of coupling molecules to plasmonic structures holds great promise towards studying weakly fluorescent, natural molecular systems. In particular it enables further, detailed study of the energy transfer processes and the role of quantum coherence at the level of single complexes.

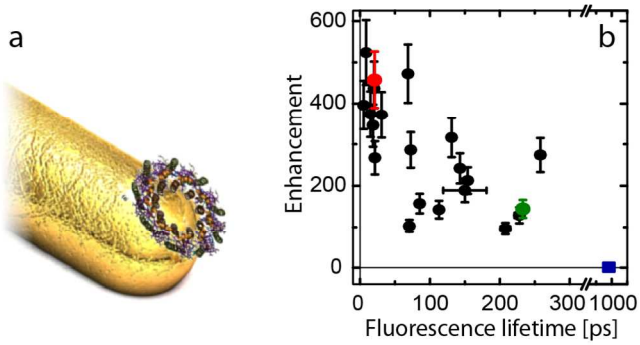

Figure 10. (a) Artist impression of a single LH2 complex coupled to a gold plasmonic antenna at the location of the plasmonic hotspot. (b) Enhancement factor as a function of fluorescence lifetime for a number of investigated individual LH2 complexes; blue reference point for free LH2 complex without plasmonic antenna.

Conclusions and outlook

We have shown that a broadband Fourier-limited pulse focused in a diffraction-limited spot is a perfect basis to probe and control individual nano-objects such as plasmonic nanoantennas and individual molecular systems. Addressing plasmonic resonances, their spectral phase response is retrieved and exploited to control the spectral response or produce dynamic nanoscale hotspots. Turning to molecular systems, the whole toolbox of coherent control is brought to single units, allowing us to prepare coherent states and trace coherent energy transfer even of complex molecular systems in a highly inhomogeneous environment.

In all these experiments control and stability of the spectral phase of the pulse has turned out to be crucially important. Measuring coherent effects in energy transfer processes or intrinsic coherences within vibrational wave-packets, the complexity of the system and its environment produce a large heterogeneity in the extracted timescales and magnitudes. Similarly for plasmonic structures, despite great advances in nanofabrication, no two plasmonic structures are identical leading to distinct heterogeneity in coherent response between these structures. Therefore pulses have to be controlled with high precision in order to probe the inhomogeneities between individual nanoparticles and not the uncertainty in spectral phase of the pulse.

In the presented experiments, to keep control and avoid artifacts, we probed the coherences using pulses with flat spectral phase and intensity given by the laser spectrum. Alternatively one could shape the laser pulse in terms of spectral intensity and phase relation to address optimally specific levels and influence chosen processes. Ultimately one could aim for closed loop coherent control on a single unit, which is quite challenging in the case of molecules emitting only a limit numbers of photons before photo bleaching.[74]

We have shown that one can independently prepare the molecule in specific coherent state and probe its coherent energy transfer and relaxation pathways. It would be truly groundbreaking if the two experiments could be combined together in a three-pulse experiment: preparing a certain designed superposition of states and next manipulate its temporal evolution towards the anticipated final state.

Detailed knowledge of the spatio-temporal coherent response of plasmonic structures is essential to design more complex plasmonic architectures capable of localizing electric fields in a nanovolume with tailored temporal and phase character. Such design brings us a step closer towards the realization of pump-probe schemes on the nanoscale. For ultrafast nanoscopy experiments on individual molecules the sample concentration is not so critical, as the local enhancement in the engineered nanovolume will dominate the detected signal. For more complex and dense molecular samples, such as bacterial membranes in which spatial coherent energy transfer amongst various complexes is expected, the perspective to exert a coherent pump-probe experiment on a chosen complex, or between two complexes, is truly fascinating.

Unfortunately all the presented experiments suffer from the fundamentally limited photostability of individual fluorescent molecules. Moreover some experimental concepts require saturating excitation conditions, while some molecules are intrinsically designed for energy transfer and avoid spontaneous emission (LH2). In spite of those limits the detection of fluorescence is still winning over alternative detection schemes in terms of simplicity of the experiment and the achievable signal-to-background ratio. Also, while relying on an incoherent detection scheme, we have demonstrated that the coherent properties of individual nanoparticles can be successfully accessed by dedicated control of the excitation path. The limitations of the presented experiments can be partially lifted by coupling molecular systems to plasmonic antennas, which speed up the radiative decay rate, resulting in a higher quantum efficiency and photon stream, combined with reduced bleaching and higher total number of photons emitted. Still detection of a coherent response would be preferred, such as absorption, stimulated emission or four-wave mixing, yet detection of single units along these routes is equally challenging.

Clearly ultrafast nanophotonics is a field in action. This review provides a timely snapshot, and surely significant advances can be expected in the near future.

AUTHOR INFORMATION

Corresponding Authors

Email:
Niek.vanHulst@ICFO.eu; Lukasz.Piatkowski@ICFO.es

Notes

The authors declare no competing financial interest.

ACKNOWLEDGMENTS

The authors would like to gratefully acknowledge all the members of the van Hulst group and collaborators, who contributed to this work, past and present. L.P. acknowledges financial support from the Marie-Curie International Fellowship COFUND and the ICFOnest program. N.F.v.H.

acknowledges the financial support by the European Commission (ERC Advanced Grants 247330-NanoAntennas and 670949-LightNet), Spanish MINECO (PlanNacional project FIS2012-35527, network FIS2014-55563-REDC and Severo Ochoa grant SEV2015-0522), the Catalan AGAUR (2014 SGR01540) and Fundació CELLEX (Barcelona).

REFERENCES

(1) Moerner, W. E.; Orrit, M. Illuminating single molecules in condensed matter. *Science* **1999**, *12*, 1670-1676.
(2) Xie, X. S.; Trautman, J. K. Optical studies of single molecules at room temperature. *Annu. Rev. Phys. Chem.* **1998**, *49*, 441-480.
(3) Xie, X. S. Single molecule spectroscopy and dynamics. *Acc. Chem. Res.* **1996**, *29*, 598-606.
(4) Moerner, W. E. A dozen years of single-molecule spectroscopy in physics, chemistry, and biophysics. *J. Phys. Chem. B* **2002**, *106*, 910-927.
(5) Tamarat, P.; Maali, A.; Lounis, B.; Orrit, M. Ten years of single-molecule spectroscopy. *J. Phys. Chem. A* **2000**, *104*, 1-16.
(6) De Schryver, F. C.; De Feyter, S.; Schweitzer, G.: *Femtochemistry*; Wiley-VCH, 2001. pp. 267.
(7) Berera, R.; van Grondelle, R.; Kennis, J. T. M. Ultrafast transient absorption spectroscopy: principles and application to photosynthetic systems. *Photosynth. Res.* **2009**, *101*, 105-118.
(8) Zewail, A. H. Femtochemistry: atomic-scale dynamics of the chemical bond using ultrafast lasers. *Angew. Chem. Int. Ed.* **2000**, *39*, 2586.
(9) Zewail, A. H. Femtochemistry: past, present, and future. *Pure Appl. Chem.* **2000**, *72*, 2219-2231.
(10) Woutersen, S.; Hamm, P. Nonlinear two-dimensional vibrational spectroscopy of peptides. *J. Phys. Condens. Matter* **2002**, *14*, 1035-1062.
(11) Guenther, T.; Lienau, C.; Elsaesser, T.; Glanemann, M.; Axt, V. M.; Kuhn, T.; Eshlaghi, S.; Wieck, A. D. Coherent nonlinear optical response of single quatum dots studied by ultrafast near-field spectroscopy. *Phys. Rev. Lett.* **2002**, *89*, 057401.
(12) van Dijk, E. M. H. P.; Hernando, J.; García-López, J.-J.; Crego-Calama, M.; Reinhoudt, D. N.; Kuipers, L.; García-Parajó, M. F.; van Hulst, N. F. Single-molecule pump-probe detection resolves ultrafast pathways in individual and coupled quantum systems. *Phys. Rev. Lett.* **2005**, *94*, 078302.
(13) Aeschlimann, M.; Bauer, M.; Bayer, D.; Brixner, T.; Cunovic, S.; Dimler, F.; Fischer, A.; Pfeiffer, W.; Rohmer, M.; Schneider, C.; Steeb, F.; Struber, C.; Voronine, D. V. Spatiotemporal control of nanooptical excitations. *Proc. Natl. Acad. Sci. U.S.A.* **2010**, *107*, 5329-5333.
(14) Aeschlimann, M.; Bauer, M.; Bayer, D.; Brixner, T.; García de Abajo, F. J.; Pfeiffer, W.; Rohmer, M.; Spindler, C.; Steeb, F. Adaptive subwavelength control of nano-optical fields. *Nature* **2007**, *446*, 301-304.
(15) Aeschlimann, M.; Brixner, T.; Fischer, A.; Kramer, C.; Melchior, P.; Pfeiffer, W.; Schneider, C.; Strüber, C.; Tuchscherer, P.; Voronine, D. V. Coherent Two-Dimensional Nanoscopy. *Science* **2011**, *333*, 1723-1726.
(16) Brixner, T.; Garcia de Abajo, F. J.; Schneider, J.; Pfeiffer, W. Nanoscopic ultrafast space-time-resolved spectroscopy. *Phys. Rev. Lett.* **2005**, *95*, 093901.
(17) Huang, J. S.; Voronine, D. V.; Tuchscherer, P.; Brixner, T.; Hecht, B. Deterministic spatiotemporal control of optical fields in nanoantennas and plasmonic circuits. *Phys Rev B* **2009**, *79*, 195441.
(18) Rewitz, C.; Keitzl, T.; Tuchscherer, P.; Huang, J. S.; Geisler, P.; Razinskas, G.; Hecht, B.; Brixner, T. Ultrafast plasmon propagation in nanowires characterized by far-field spectral interferometry. *Nano Lett.* **2012**, *12*, 45-49.
(19) Kravtsov, V.; Ulbricht, R.; Atkin, J. M.; Raschke, M. B. Plasmonic nanofocused four-wave mixing for femtosecond near-field imaging. *Nat. Nanotechnol.* **2016**.
(20) Anderson, A.; Deryckx, K. S.; Xu, X. G.; Steinmeyer, G. n.; Raschke, M. B. Few-Femtosecond Plasmon Dephasing of a Single Metallic Nanostructure from Optical Response Function Reconstruction by Interferometric Frequency Resolved Optical Gating. *Nano Lett.* **2010**, *10*, 2519-2524.
(21) Yampolsky, S.; Fishman, D. A.; Dey, S.; Hulkko, E.; Banik, M.; Potma, E. O.; Apkarian, V. A. Seeing a single molecule vibrate through time-resolved coherent anti-stokes raman scttering. *Nat. Photon.* **2014**, *8*, 650-656.
(22) Unold, T.; Müller, K.; Lienau, C.; Elsaesser, T.; Eshlaghi, S.; Wieck, A. D. Optical Stark effect in a quantum dot: ultrafast polarization control of single exciton. *Phys. Rev. Lett.* **2004**, *92*, 157401.
(23) Vasa, P.; Wang, W.; Pomraenke, R.; Lammers, M.; Maiuri, M.; Manzoni, C.; Cerullo, G.; Lienau, C. Real-time observation of ultrafast Rabi oscillations between excitons and plasmons in metal nanostructures with J-aggregates. *Nat. Photon.* **2013**, *7*, 128-132.
(24) Vasa, P.; Ropers, C.; Pomraenke, R.; Lienau, C. Ultra-fast nano-optics. *Laser Photon. Rev.* **2009**, *3*, 483-507.
(25) Lienau, C.; Elsaesser, T.: Ultrafast coherent spectroscopy of single semiconductor quantum dots. In *Semiconductor Nanostructures (Nanoscience and Technology)*; 1 ed.; Bimberg, D., Ed.; Springer-Verlag, 2008.
(26) van Dijk, E. M. H. P.; Hernando, J.; García-Parajó, M. F.; van Hulst, N. F. Single-molecule pump-probe expriments reveal variations in ultrafast energy redistribution. *J. Chem. Phys.* **2005**, *123*, 064703.
(27) Brinks, D.; Hildner, R.; van Dijk, E. M. H. P.; Stefani, F. D.; Nieder, J. B.; Hernando, J.; van Hulst, N. F. Ultrafast dynamics of single molecules. *Chem. Soc. Rev.* **2014**, *43*, 2476-2491.
(28) Brinks, D.; Hildner, R.; Stefani, F. D.; van Hulst, N. F. Beating spatio-temporal coupling: implications for pulse shaping and coherent control experiments. *Opt. Express* **2011**, *19*, 26486-26499.
(29) Brinks, D.; Hildner, R.; Stefani, F. D.; van Hulst, N. F. Coherent control of single molecules at room temperature. *Faraday Discuss.* **2011**, *153*, 51-60.
(30) Brinks, D.; Stefani, F. D.; Kulzer, F.; Hildner, R.; Taminiau, T. H.; Avlasevich, Y.; Mullen, K.; van Hulst, N. F. Visualizing and controlling vibrational wave packets of single molecules. *Nature* **2010**, *465*, 905-908.
(31) Hildner, R.; Brinks, D.; Nieder, J. B.; Cogdell, R. J.; van Hulst, N. F. Quantum coherent energy transfer over varying pathways in single light-harvesting complexes. *Science* **2013**, *340*, 1448-1451.
(32) Hildner, R.; Brinks, D.; van Hulst, N. F. Femtosecond coherence and quantum control of single molecules at room temperature. *Nature Phys.* **2011**, *7*, 172-177.
(33) Brinks, D.; Castro-Lopez, M.; Hildner, R.; van Hulst, N. F. Plasmonic antennas as design elements for coherent ultrafast nanophotonics. *Proc. Natl. Acad. Sci. U.S.A.* **2013**, *110*, 18386-18390.
(34) Accanto, N.; Nieder, J. B.; Piatkowski, L.; Castro-Lopez, M.; Pastorelli, F.; Brinks, D.; van Hulst, N. F. Phase control of femtosecond pulses on the nanoscale using second harmonic nanoparticles. *Light Sci. Appl.* **2014**, *3*, e143.
(35) Accanto, N.; Piatkowski, L.; Hancu, I. M.; Renger, J.; van Hulst, N. F. Resonant plasmonic nanoparticles for multicolor second harmonic imaging. *Appl. Phys. Lett.* **2016**, *in press*.
(36) Accanto, N.; Piatkowski, L.; Renger, J.; van Hulst, N. F. Capturing the optical phase response of nanoantennas by coherent second-harmonic microscopy. *Nano Lett.* **2014**, *14*, 4078-4082.
(37) Shapiro, M.; Brumer, P.: *Principles of the Quantum Control of Molecular Processes*, 2003.
(38) Brif, C.; Chakrabarti, R.; Rabitz, H. Control of quantum phenomena: past, present and future. *New J Phys* **2010**, *12*, 075008.
(39) Judson, R. S.; Rabitz, H. Teaching Lasers to Control Molecules. *Phys. Rev. Lett.* **1992**, *68*, 1500-1503.
(40) Dantus, M.; Lozovoy, V. V. Experimental coherent laser control of physicochemical processes. *Chem. Rev.* **2004**, *104*, 1813-1859.
(41) Nuernberger, P.; Vogt, G.; Brixner, T.; Gerber, G. Femtosecond quantum control of molecular dynamics in the condensed phase. *Phys. Chem. Chem. Phys.* **2007**, *9*, 2470-2497.
(42) Silberberg, Y. Quantum coherent control for nonlinear spectroscopy and microscopy. *Annu. Rev. Phys. Chem.* **2009**, *60*, 277-292.
(43) Rosker, M. J.; Wise, F. W.; Tang, C. L. Femtosecond relaxation dynamics of large molecules. *Phys. Rev. Lett.* **1986**, *57*, 321-324.
(44) Xie, X. S.; Trautman, J. K. Optical studies of single molecules at room temperature. *Annu. Rev. Phys. Chem.* **1998**, *49*, 441-480.
(45) Vallée, R. A. L.; Tomczak, N.; Kuipers, L.; Vancso, G. J.; van Hulst, N. F. Single molecule lifetime fluctuations reveal segmental dynamics in polymers. *Phys. Rev. Lett.* **2003**, *91*, 038301.
(46) Nie, S.; Chiu, D. T.; Zare, R. N. Probing individual molecules with confocal fluorescence microscopy. *Science* **1994**, *266*, 1018-1021.
(47) Fourkas, J. T.; Berg, M. Temperature-dependent ultrafast solvation dynamics ina completely nonpolar system. *J. Chem. Phys.* **1993**, *98*, 7773.
(48) Bagchi, B. Molecular theory of nonpolar solvation dynamics. *J. Chem. Phys.* **1994**, *100*, 6658.

(49) Dyba, M.; Hell, S. W. Focal spots of size λ/33 open up far-field fluorescence microscopy at 33 nm axial resolution. *Phys. Rev. Lett.* **2002**, *88*, 163901.
(50) Kastrup, L.; Hell, S. W. Absolute optical cross section of individual fluorescent molecules. *Angew. Chem. Int. Ed.* **2004**, *43*, 6646-6649.
(51) Orrit, M. Photon statistics in single molecule experiments. *Single Mol.* **2002**, *3*, 255-265.
(52) Fuchs, U.; Zeitner, U.; Tünnermann, A. Ultra-short pulse propagation in complex optical systems. *Opt. Express* **2005**, *13*, 3852-3861.
(53) Trebino, M. Measuring the seemingly immeasurable. *Nat. Photon.* **2011**, *5*, 189-192.
(54) Iaconis, C.; Walmsley, I. A. Spectral phase interferometry for direct electric-field reconstruction of ultrashort optical pulses. *Opt. Lett.* **1998**, *23*, 792-794.
(55) Xu, B.; Gunn, J. M.; Cruz, J. M. D.; Lozovoy, V. V.; Dantus, M. Quantitative investigation of the multiphoton intrapulse interference phase scan method for simultaneous phase measurement and compensation of femtosecond laser pulses. *J. Opt. Soc. Am. B* **2006**, *23*, 750-759.
(56) Extermann, J.; Bonacina, L.; Courvoisier, F.; Kiselev, D.; Mugnier, Y.; Le Dantec, R.; Galez, C.; Wolf, J.-P. Nano-FROG: Frequency resolved optical gating by a nanometric object. *Opt. Express* **2008**, *16*, 10405-10411.
(57) Weiner, A. M. Femtosecond pulse shaping using spatial light modulators. *Rev. Sci. Instrum.* **2000**, *71*, 1929-1960.
(58) Monmayrant, A.; Weber, S.; Chatel, B. A newcomer's guide to ultrashort pulse shaping and characterization. *J. Phys. B: At. Mol. Opt. Phys.* **2010**, *43*, 1-34.
(59) McCabe, D. J.; Austin, D. R.; Tajalli, A.; Weber, S.; Walmsley, I. A.; Chatel, B. Space-time coupling of shaped ultrafast ultraviolet pulses from an acousto-optic programmable dispersive filter. *J. Opt. Soc. Am. B* **2011**, *28*, 58-64.
(60) Martinez, O. E. Grating and prism compressors in the case of finite beam size. *J. Opt. Soc. Am. B* **1986**, *3*, 929-934.
(61) Strickland, D.; Mourou, G. Compression of amplified chirped optical pulses. *Opt. Commun.* **1985**, *56*, 219-221.
(62) Biagioni, P.; Huang, J. S.; Hecht, B. Nanoantennas for visible and infrared radiation. *Rep. Prog. Phys.* **2012**, *75*, 024402.
(63) Novotny, L.; van Hulst, N. Antennas for light. *Nature Photon.* **2011**, *5*, 83-90.
(64) Stockman, M. I.; Faleev, S. V.; Bergman, D. J. Coherent control of femtosecond energy localization in nanosystems. *Phys. Rev. Lett.* **2002**, *88*, 067402.
(65) Hanke, T.; Cesar, J.; Knittel, V.; Trugler, A.; Hohenester, U.; Leitenstorfer, A.; Bratschitsch, R. Tailoring spatiotemporal light confinement in single plasmonic nanoantennas. *Nano Lett.* **2012**, *12*, 992-996.
(66) Nishiyama, Y.; Imaeda, K.; Imura, K.; Okamoto, H. Plasmon Dephasing in Single Gold Nanorods Observed By Ultrafast Time-Resolved Near-Field Optical Microscopy. *J. Phys. Chem. C* **2015**, *119*, 16215--16222.
(67) Sun, Q.; Ueno, K.; Yu, H.; Kubo, A.; Matsuo, Y.; Misawa, H. Direct imaging of the near field and dynamics of surface plasmon resonance on gold nanostructures using photoemission electron microscopy. *Light Sci. Appl.* **2013**, *2*, e118.
(68) Mårsell, E.; Losquin, A.; Svrd, R.; Miranda, M.; Guo, C.; Harth, A.; Lorek, E.; Mauritsson, J.; Arnold, C. L.; Xu, H.; Lhuillier, A.; Mikkelsen, A. Nanoscale Imaging of Local Few-Femtosecond Near-Field Dynamics within a Single Plasmonic Nanoantenna. *Nano Lett.* **2015**, *15*, 6601--6608.
(69) Pantazis, P.; Maloney, J.; Wu, D.; Fraser, S. E. Second harmonic generating (SHG) nanoprobes for in vivo imaging. *Proc. Natl. Acad. Sci. U.S.A.* **2010**, *107*, 14535--14540.
(70) Staedler, D.; Magouroux, T.; Hadji, R.; Joulaud, C.; Extermann, J.; Schwung, S.; Passemard, S.; Kasparian, C.; Clarke, G.; Gerrmann, M.; Dantec, R. L.; Mugnier, Y.; Rytz, D.; Ciepielewski, D.; Galez, C.; Gerber-Lemaire, S.; Juillerat-Jeanneret, L.; Bonacina, L.; Wolf, J.-P. Harmonic Nanocrystals for Biolabeling: A Survey of Optical Properties and Biocompatibility. *ACS nano* **2012**, *6*, 2542--2549.
(71) Kamada, H.; Gotoh, H.; Temmyo, J.; Takagahara, T.; Ando, H. Exciton Rabi oscillations in a single quantum dot. *Phys. Rev. Lett.* **2001**, *87*, 246401.
(72) Wrigge, G.; Gerhardt, I.; Hwang, J.; Zumofen, G.; Sandoghdar, V. Efficient coupling of photons to a single molecule and the observation of its resonance fluorescence. *Nature Phys.* **2008**, *6*, 60-66.
(73) Schweitzer, G.; Gronheid, R.; Jordens, S.; Lor, M.; De Belder, G.; Weil, T.; Reuther, E.; Müllen, K.; De Schryver, F. C. Intramolecular directional energy transfer processes in dendrimers containing perylene and terrylene chromophores. *J. Phys. Chem. A* **2003**, *107*, 3199-3207.
(74) Avlasevich, Y.; Müller, S.; Erk, P.; Müllen, K. Novel core-expanded rylenebis(dicarboximide) dyes bearing pentacene units: facile synthesis and photophysical properties. *Chem. Eur. J.* **2007**, *13*, 6555-6561.
(75) Scherer, N. F.; Carlson, R. J.; Matro, A.; Du, M.; Ruggiero, A. J.; Romero-Rochin, V.; Cina, J. A.; Fleming, G. R. Fluorescence-detected wave packet interferometry: time resolved molecular spectroscopy with sequences of femtosecond phase-locked pulses. *J. Chem. Phys.* **1991**, *95*, 1487-1512.
(76) Piatkowski, L.; Gellings, E.; van Hulst, N. F. Broadband single-molecule excitation spectroscopy. *Nature Commun.* **2016**, *7*, 10411.
(77) Weigel, A.; Sebesta, A.; Kukura, P. Shaped and feedback-controlled excitation of single molecules in the weak-field limit. *J. Phys. Chem. Lett.* **2015**.
(78) Scholes, G. D. Quantum-coherent electronic energy transfer: did nature think of it first? *J. Phys. Chem. Lett.* **2010**, *1*, 2-8.
(79) Engel, G. S.; Calhoun, T. R.; Read, E. L.; Ahn, T.-K.; Mancal, T.; Cheng, Y.-C.; Blankenship, R. E.; Fleming, G. R. Evidence for wavelike energy transfer through quantum coherence in photosynthetic systems. *Nature* **2007**, *446*, 782-786.
(80) Collini, E.; Wong, C. Y.; Wilk, K. E.; Curmi, P. M. G.; Brumer, P.; Scholes, G. D. Coherently wired light-harvesting in photosynthetic marine algae at ambient temperature. *Nature* **2010**, *463*, 644-647.
(81) Cogdell, R. J.; Gall, A.; Köhler, J. The architecture and function of the light-harvesting apparatus of purple bacteria: from single molecule to in vivo membranes. *Rev. Biophys.* **2006**, *39*, 227-324.
(82) McDermott, G.; Prince, S. M.; Freer, A. A.; Hawthornthwaite-lawless, A. M.; Papiz, M. Z.; Cogdell, R. J.; Isaacs, N. W. Crystal-structure of an integral membrane light- harvesting complex from photosynthetic bacteria. *Nature* **1995**, *374*, 517-521.
(83) Fromm, D. P.; Sundaramurthy, A.; Schuck, P. J.; Kino, G.; Moerner, W. E. Gap-dependent optical coupling of single 'Bowtie' nanoantennas resonant in the visible. *Nano Lett.* **2004**, *4*, 957-961.
(84) Mühlschlegel, P.; Eisler, H. J.; Martin, O. J.; Hecht, B.; Pohl, D. W. Resonant optical antennas. *Science* **2005**, *308*, 1607-1609.
(85) Farahani, J. N.; Pohl, D. W.; Eisler, H. J.; Hecht, B. Single quantum dot coupled to a scanning optical nanoantenna: a tunable superemitter. *Phys. Rev. Lett.* **2005**, *95*, 017402.
(86) Wientjes, E.; Renger, J.; Curto, A. G.; Cogdell, R. J.; van Hulst, N. F. Strong antenna-enhanced fluorescence of a single light-harvesting complex shows photon antibunching. *Nature Commun.* **2014**, *5*, 4236.

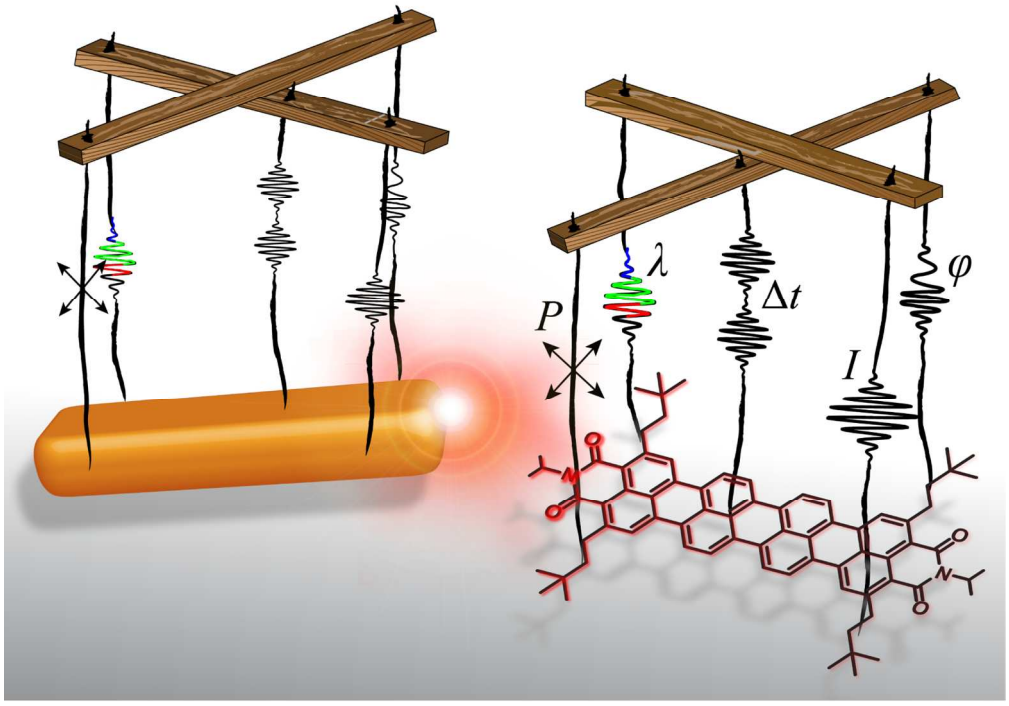

Figure 1, revised
141x99mm (300 x 300 DPI)

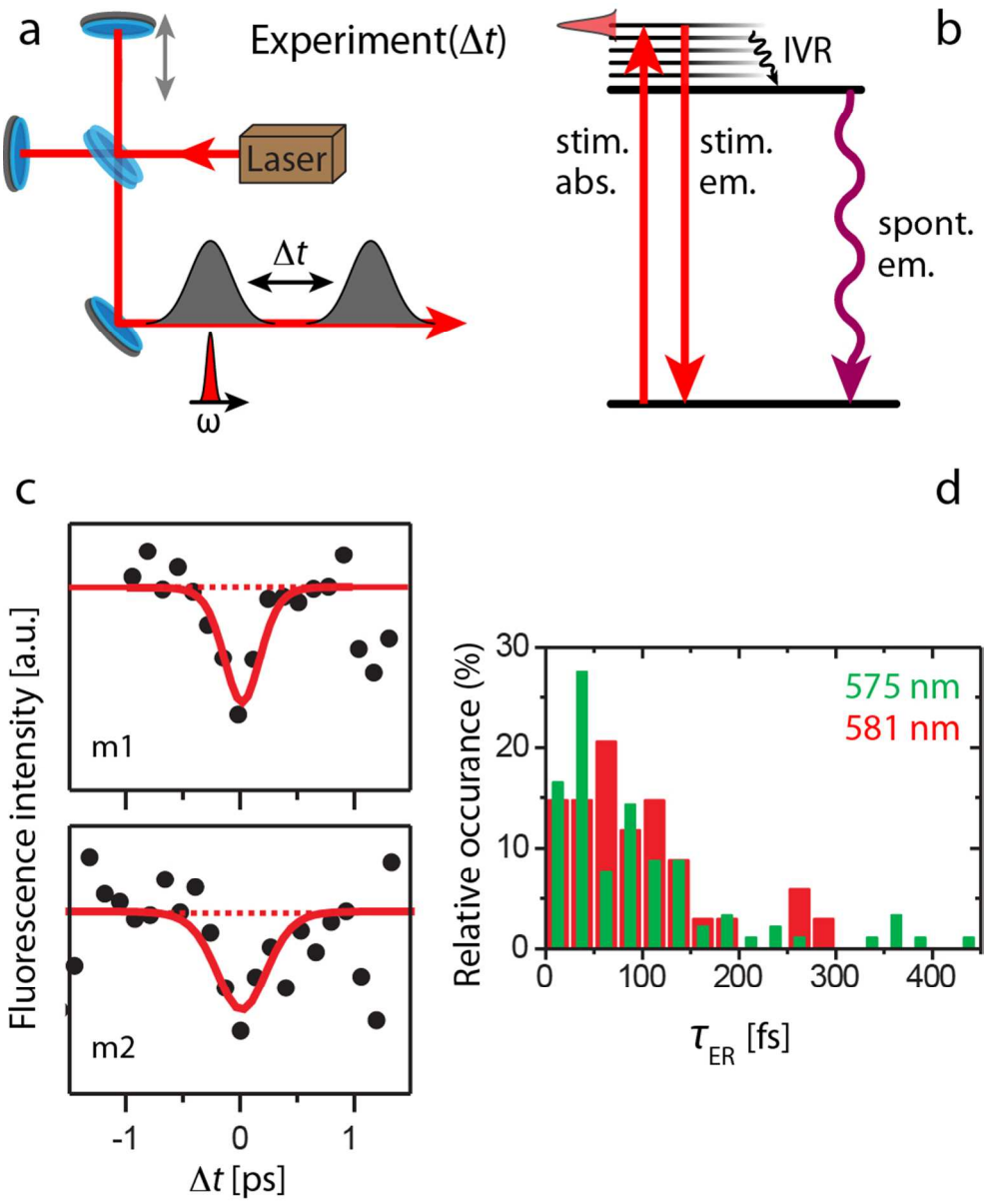

Figure 2
84x102mm (300 x 300 DPI)

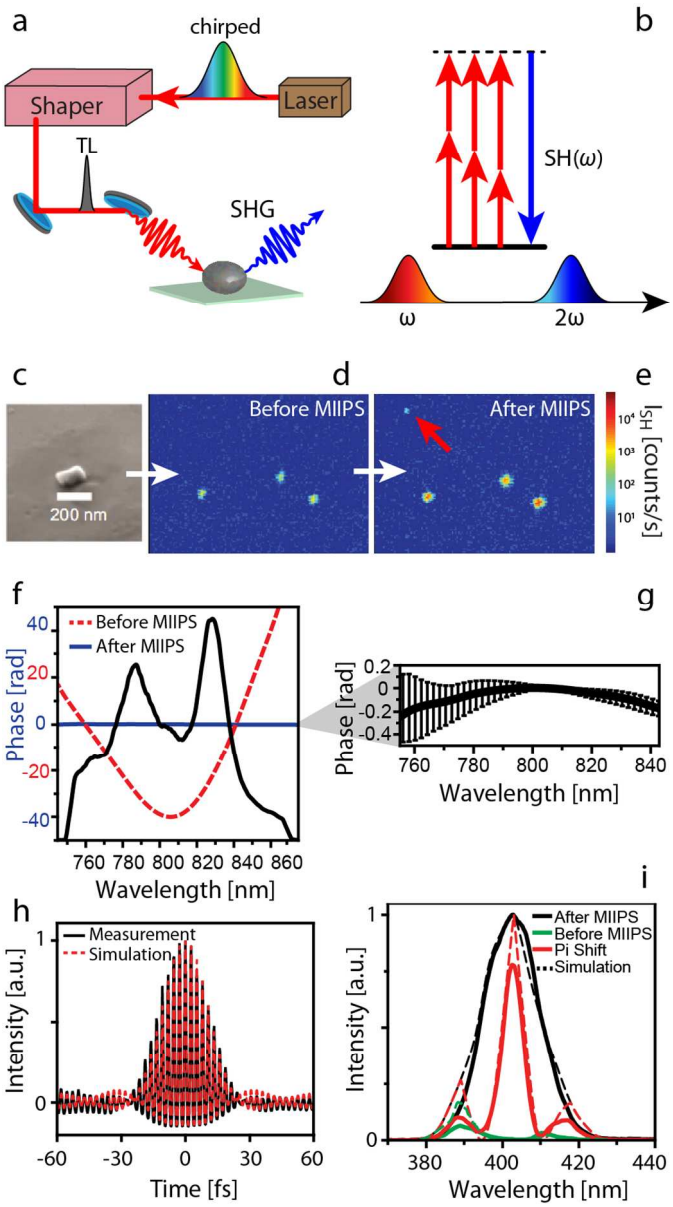

Figure 3
84x152mm (300 x 300 DPI)

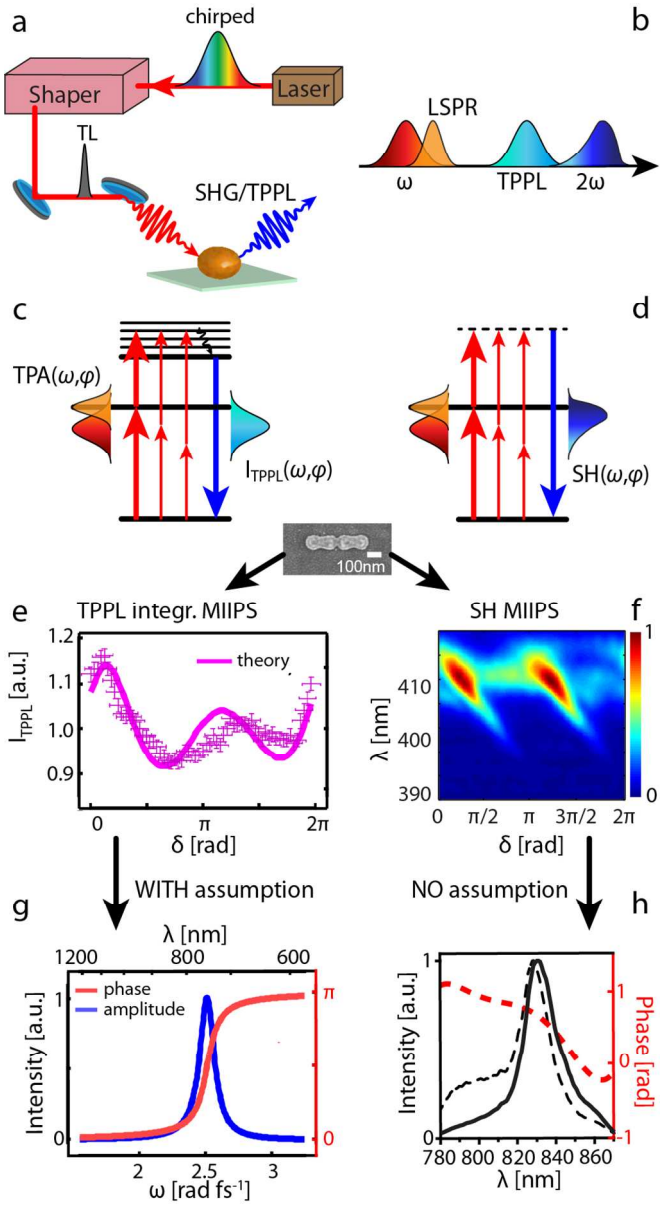

Figure 4
85x155mm (300 x 300 DPI)

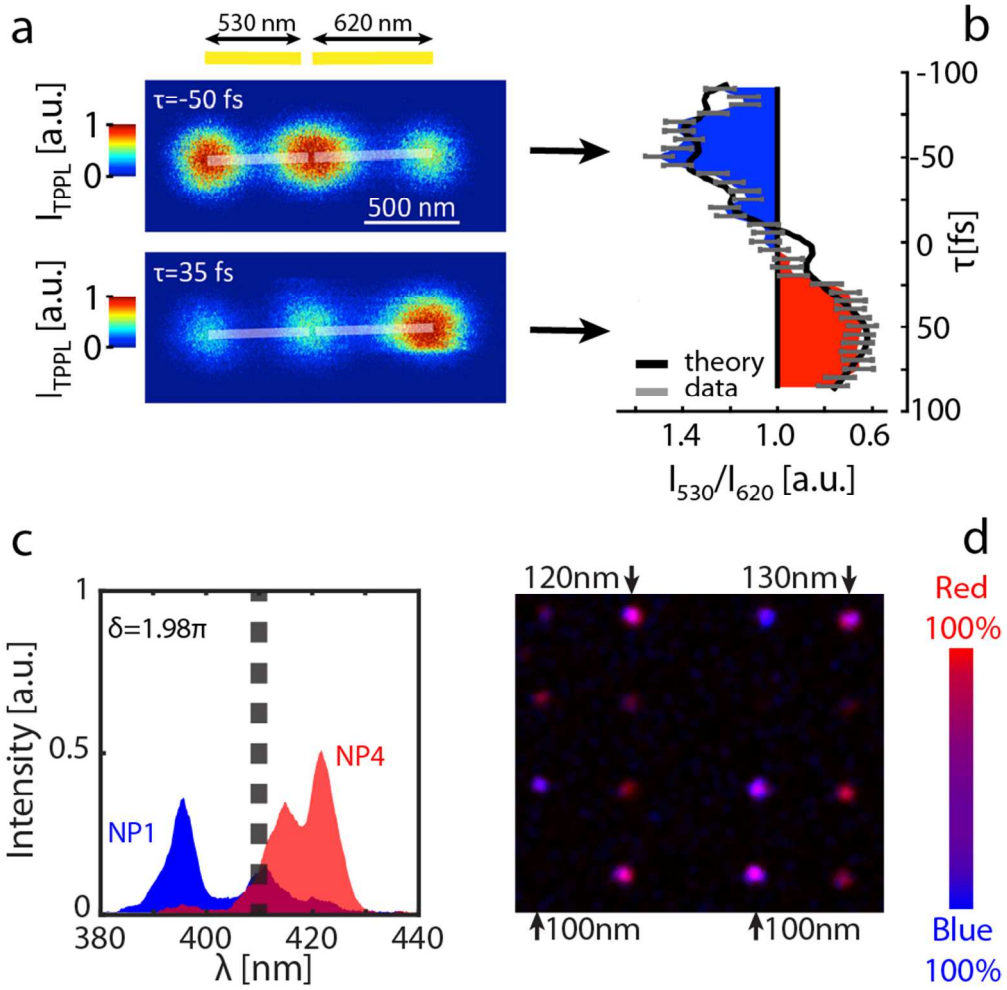

Figure 5
84x83mm (300 x 300 DPI)

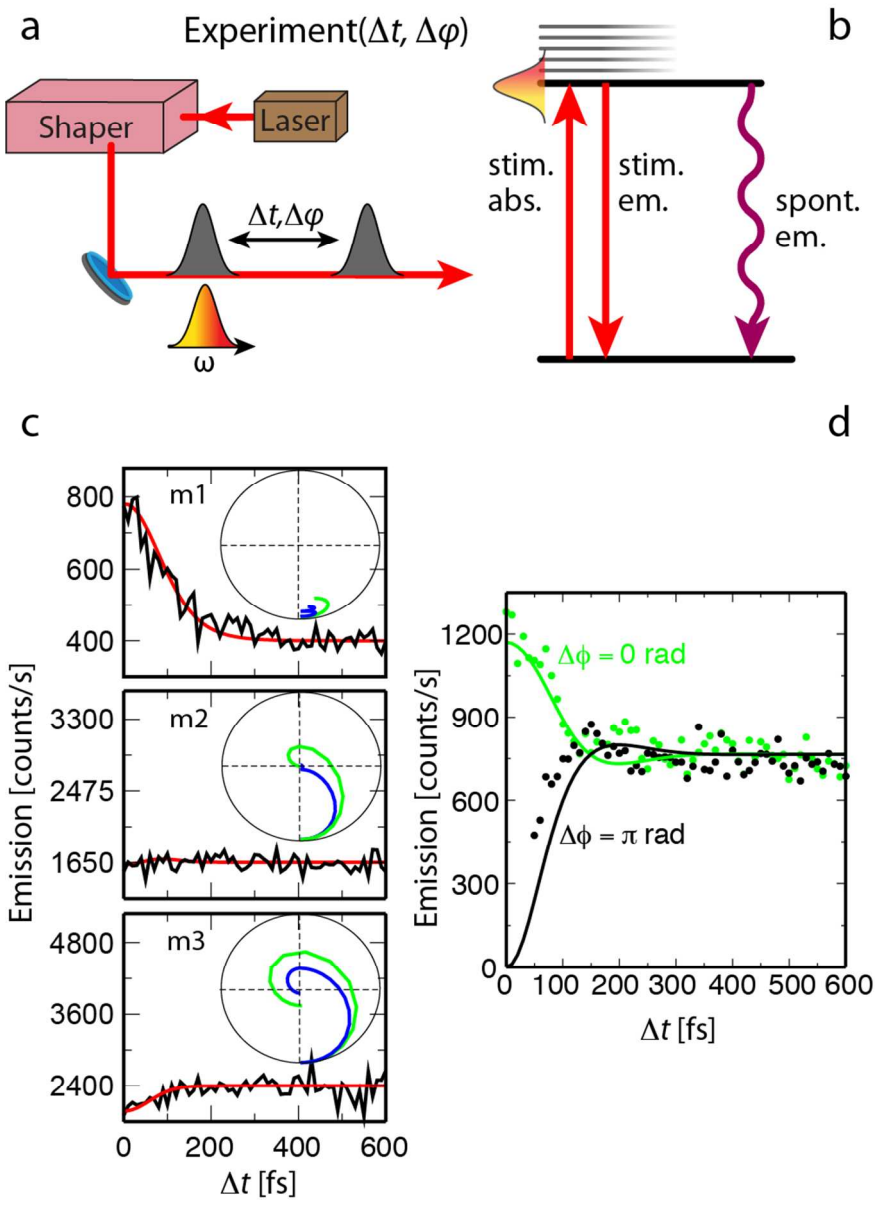

Figure 6
84x117mm (300 x 300 DPI)

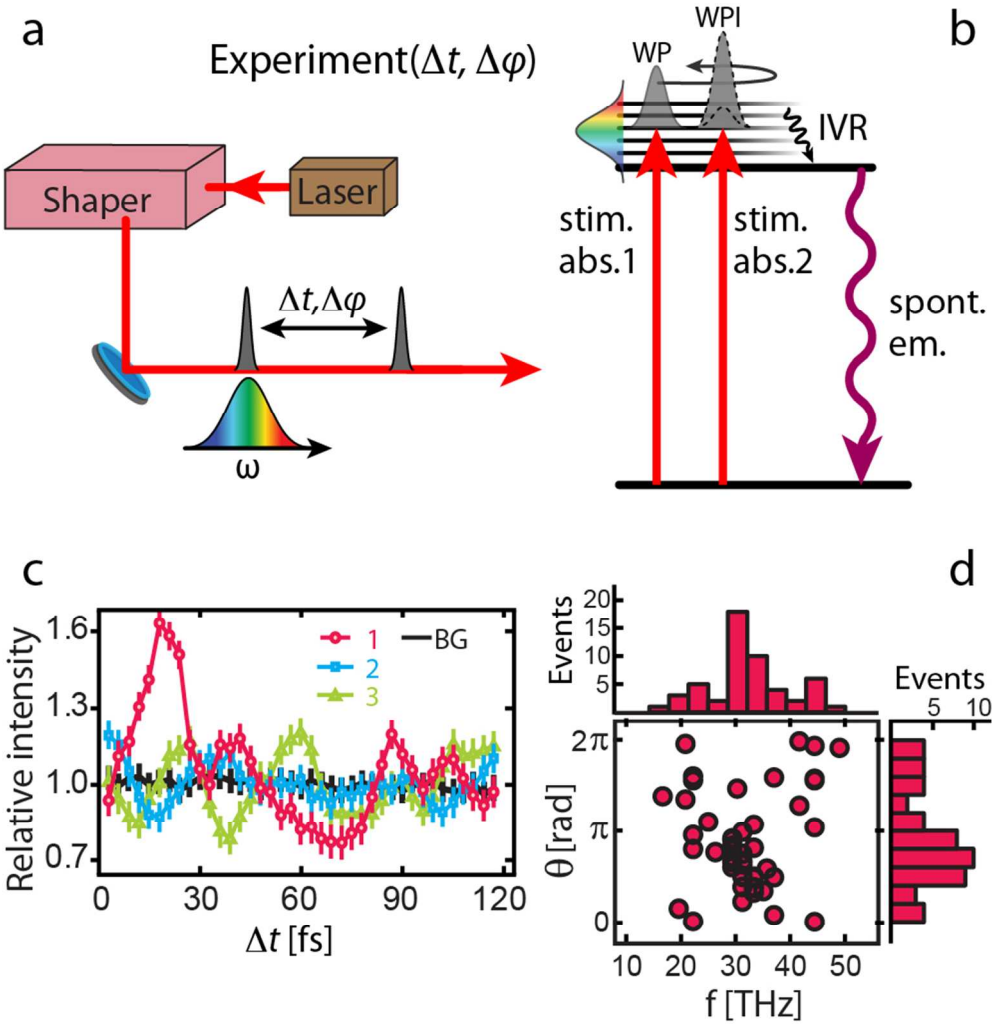

Figure 7
85x86mm (300 x 300 DPI)

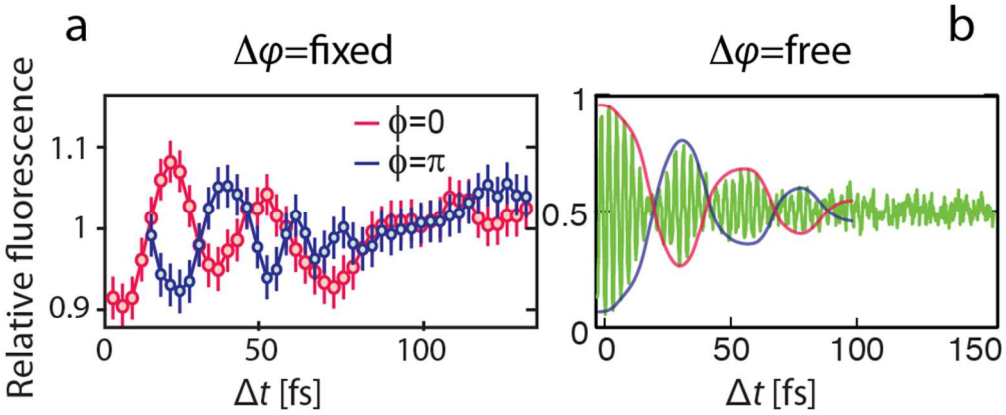

Figure 8
84x35mm (300 x 300 DPI)

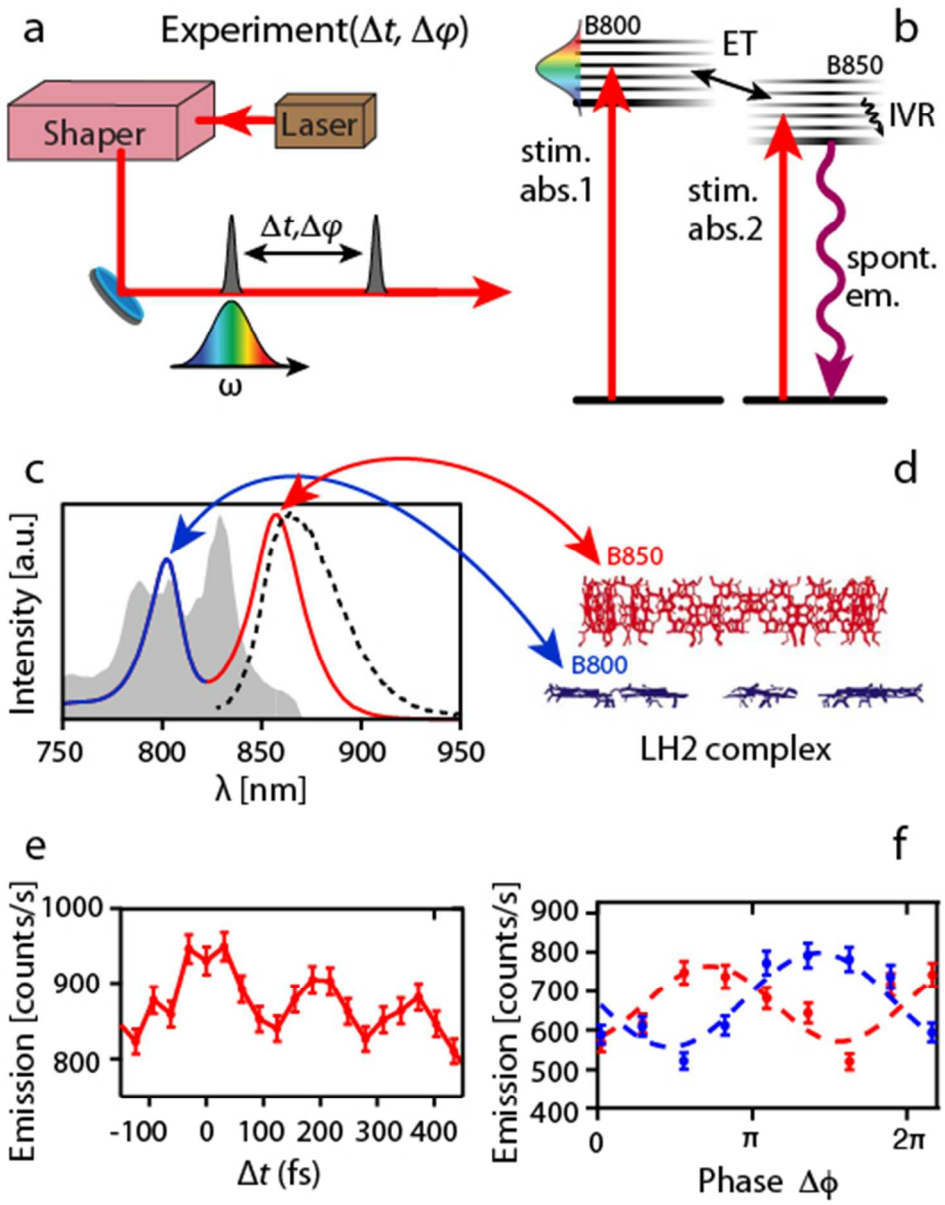

Figure 9 revised
85x108mm (150 x 150 DPI)

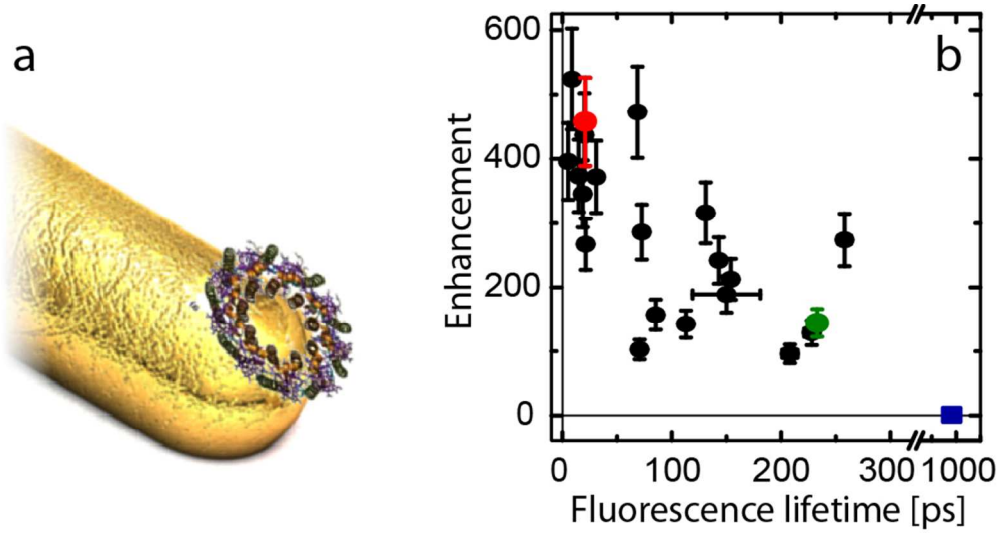

Figure 10
84x45mm (300 x 300 DPI)

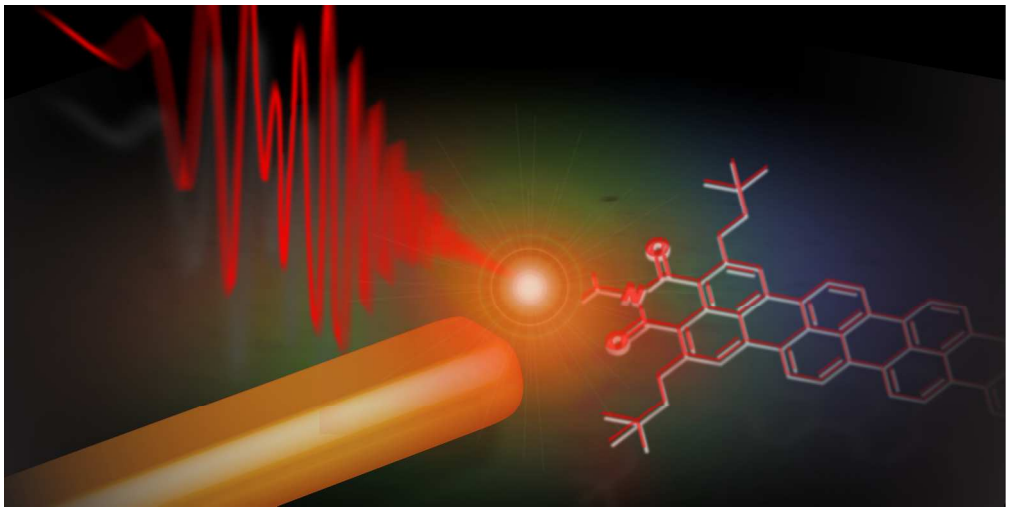

TOC figure
300x150mm (300 x 300 DPI)